OXIDATIVE DEHYDROGENATION OF N-BUTANE TO 1,3-BUTADIENE OVER BIMETALLIC BI-NI OXIDE SUPPORTED CATALYSTS

BY

OMER ELMUTASIM ELMAHADI ELFAKI

A Thesis Presented to the

DEANSHIP OF GRADUATE STUDIES

KING FAHD UNIVERSITY OF PETROLEUM & MINERALS

DHAHRAN, SAUDI ARABIA

In Partial Fulfillment of the
Requirements for the Degree of

MASTER OF SCIENCE

In

CHEMICAL ENGINEERING

MAY 2017

KING FAHD UNIVERSITY OF PETROLEUM & MINERALS

DHAHRAN- 31261, SAUDI ARABIA

DEANSHIP OF GRADUATE STUDIES

This thesis, written by **Omer Elmutasim Elmahadi Elfaki** under the direction his thesis advisor and approved by his thesis committee, has been presented and accepted by the Dean of Graduate Studies, in partial fulfillment of the requirements for the degree of

MASTER OF SCIENCE IN CHEMICAL ENGINEERING

Dr. Mohammed Ba-Shammakh
Department Chairman

Dr. Sulaiman Al-Khattaf
(Advisor)

Dr. Salam A. Zummo
Dean of Graduate Studies

عمادة الدراسات العليا
DEANSHIP OF GRADUATE STUDIES

Dr. Mohammed Ba-Shammakh
(Member)

2/5/17
Date

Dr. Isam Al-jundi
(Member)

Dedicated to my parents,

sisters and brother for their immeasurable love and support throughout my entire life.

ACKNOWLEDGMENTS

First and foremost, I am grateful to Allah (SWT), the Lord of the worlds, for giving me life to accomplish this far. To Him belongs all praise in the Heavens and on Earth. I thank him for guiding me to this point of my career and the uncountable favours he has bestowed on me.

Thereafter, I would like to express my deepest gratitude to my thesis advisor Dr. Sulaiman Al-Khattaf, for his excellent guidance, inspiration and motivation. I am very thankful for his support academically and emotionally. I would like to thank the members of my committee, Dr. Isam Al-jundi for the immense assistance he provided at all levels of the research project and Dr. Mohammed Ba-Shammakh for valuable suggestions throughout this work.

To my parents, brother and sisters, I am deeply appreciative of your patience, encouragement and love throughout the study.

TABLE OF CONTENTS

LIST OF TABLES

LIST OF FIGURES

LIST OF ABBREVIATIONS

ODH	:	Oxidative Dehydrogenation
BD	:	Butadiene
OC	:	Oxygenate and Cracking
PO	:	Partial Oxidation
GHSV	:	Gas Hourly Space Velocity
GC	:	Gas Chromatographic
FID	:	Flame Ionized Detector
TCD	:	Thermal Conductivity Detector
XRD	:	X-ray Diffraction
BET	:	Brunauer Emmett-Teller
BJH	:	Barrett-Joyner-Halenda
TPD	:	Temperature Programmed Desorption
TPR	:	Temperature Programmed Reduction
$\boldsymbol{k_{i0}}$	:	Pre-exponential factor of the reaction i
$\boldsymbol{E_i}$	:	Activation energy of the reaction i

$\boldsymbol{Y_i}$	:	Mole fraction of lump *i*
T	:	Reaction temperature
$\mathbf{T_o}$	:	Average temperature of the experiments
R	:	Universal gas constant
SS	:	Sum of Squares

ABSTRACT

Full Name : Omer Elmutasim Elmahadi Elfaki

Thesis Title : Oxidative Dehydrogenation of n-butane to 1,3-Butadiene Over Bimetallic Bi-Ni Oxide Supported Catalysts

Major Field : Chemical Engineering

Date of Degree : May, 2017

The influence of different supports such as TiC, SiC and silicalite on the catalytic performance of bimetallic Bi-Ni oxide supported catalysts for the oxidative dehydrogenation of *n*-butane (hereafter named ODH) to *1,3*-butadiene was investigated. The co-impregnation technique was followed to synthesize all the catalysts where the metal content of Bi and Ni was maintained at 30 and 20 wt% respectively. The catalysts were characterized by BET, XRD, CO_2/NH_3-TPD and H_2-TPR measurement techniques. The catalytic evaluation showed that bimetallic Bi-NiO/ TiC catalyst exhibited the highest dehydrogenation selectivity of 83.7%, while the formation of butadiene remained at 50.7% and greater compared to butenes (33%). The selectivity to butadiene followed the sequence: Bi-Ni/TiC > Bi-Ni/SiC > Bi-Ni/Silicalite. The different supports investigated showed varying performance due to difference in their ability to interact actively with the metal species in terms of dispersion and reducibility as well as acidic/basic character. As regards Bi-NiO/ TiC, a wide range of operating parameters were investigated, including O_2/n-C_4H_{10} ratio, reaction temperature and space velocity. The Bi-Ni/TiC catalyst exhibited satisfactory stability as proven by 10 hours on stream test, where no significant catalyst deactivation was observed. The improved performance of Bi-NiO/ TiC can be ascribed to the synergetic effect of redox property, uniform

dispersion of Bi-Ni-O metal oxides over TiC and couple of strong basicity and weak acidity. Kinetic modeling was developed for the Bi-NiO/ TiC catalyst based on experiments performed in fixed bed reactor at a temperature range 350-500 ºC. MATLAB program used power law model to estimate the kinetic parameters.

ملخص الرسالة

الاسم الكامل: عمر المعتصم المهدي الفكي

عنوان الرسالة: نزع الهيدروجين المؤكسد من البيوتان لإنتاج البيوتاديين باستخدام حفازات النيكل و البزموت الثنائية المدعمة.

التخصص: هندسة كيميائية

تاريخ الدرجة العلمية:مايو 2017

تأثير المواد الحاملة مختلفة مثل :كربيد التيتانيوم، كربيد السيليكون و سيليكالايت على الاداء التحفيزي لحفازات النيكل و البزموت الثنائية لعملية نزع الهيدروجين المؤكسد من البيوتان لإنتاج البيوتاديين تمت دراستها. طريقة التحميل المشترك اتبعت لتحضير كل الحفازات، حيث أن كمية النيكل والبزموت تم تثبيتها عند 30% و 20% علي التوالي. تمت دراسة خواص الحفازات المصنعة باستخدام طريقة انكسار الاشعة السينية، الامتزاز الحراري المبرمج و الاختزال الحراري المبرمج. أوضح التقييم التحفيزي ان حفاز ثنائي النيكل و البزموت المحمول علي كربيد التيتانيوم ابدى اعلى انتقائية لنزع الهيدروجين (83.7%) ، حيث انا البيوتاديين تكون بنسبة (50.7%) و هي اعلي مقارنة مع انتقائية البيوتين (33%). ترتيب انتقائية البيوتاديين على الحوامل المختلفة هو: كربيد التيتانيوم > كربيد السيليكون > سيليكالايت. الحوامل المختلفة التي تمت دراستها اعطت أداء مختلف بسبب اختلاف قابلية كل حامل علي التفاعل مع المعادن المثبتة عليه نتيجة لاختلاف التشتت و الاختزال و الخاصية الحمضية و القاعدية. بخصوص الحفاز المحمول علي كربيد التيتانيوم، العديد من العوامل التشغيلية تمت دراستها نسبة البيوتان/الاكسجين و درجة حرارة التفاعل و السرعة. الحفاز المحمول علي كربيد التيتانيوم ابدى استقرار مقبول حسب اختبار الاستقرارية لمدة عشرة ساعات، حيث لم يلاحظ اي فقدان لنشاط الحفاز. الأداء المحسن لهذا الحفاز عُزِيً للاثر المتآزر لخاصية الاكسدة و الاختزال و التشتت المنتظم لاكاسيد المعادن، بالاضافة للقاعدية القوية و الحامضية الضعيفة. تم تطوير النماذج الحركية أستنادا على البيانات العملية لإختبار للحفاز المحمول علي كربيد التيتانيوم في مفاعل مثبت عند دراجات حرارة تتراوح من 350-500 درجة مئوية. و قد أستخدم نموذج قانون القوة لتقدير المعاملات الحركية بإستخدام برنامج .Matlab.

CHAPTER 1

INTRODUCTION

1.1 Background

The availability of light alkanes at relatively low cost compared to the unsaturated hydrocarbons and also their non-aggressive impact on the environment is providing an incentive to used them as feedstock in the petrochemical industry [1]. In Particular, the n-butane can be obtained by distillation of liquefied petroleum gas (LPG).

Nowadays, Butadiene is particularly important since it is used as feedstock for variety of synthetic polymers including “styrene butadiene rubber (SBR), acrylonitrile butadiene styrene (ABS), polybutadiene rubber (PBR), styrene butadiene latex and Nitrile rubber “, which is commonly used for the production of tires. Currently a great interest for Butadiene supply is driven to a large extent by the automotive sector.

Globally, the demand of butenes and 1,3-butadiene is expected to increase by 3% by the end of this decade [9]. In particular, the demand of ABS in China has increased significantly with growth of the electronics market. Also in Korea the butadiene demand has surpassed its supply because the production of SBR is increasing [2].

The conventional processes for producing butadiene include steam cracking process which is gas phase homogenous reaction, in which the hydrocarbon feedstock is fed to the steam cracker (Pyrolysis furnace) where it combines with steam, then heated to temperature range between 790-830 °C. At this high temperature, the feedstock

decomposes forming a wide range of hydrocarbon including olefins, di-olefins paraffin's and H_2 molecules [3]. The catalytic dehydrogenation process has two steps; initially the normal butane decomposes to butene and then to 1,3-butadiene (Houdry Catadiene process) [1] [1], [4]. In the catalytic dehydrogenation process the n-butane is dehydrogenated over Cr_2/Al_2O_3 catalyst at high temperature (600-680 °C) [3], [5].

The above-mentioned processes have the same drawbacks, as they are endothermic reactions that require large amount energy and the coke formation which causes catalyst deactivation. Additionally, the catalytic dehydrogenation reaction is thermodynamically limited to high yield of butadiene at low temperature [2], [3]. Therefore, the endothermic nature, together with the high temperature required make these processes very energy intensive. Furthermore, the selectivity control is very challenging at this high temperature [3].

The ODH process has been proposed as an alternative process for olefins and di-olefins production, it is an exothermic reaction, allows overcoming the thermodynamic restriction of the catalytic dehydrogenation process through formation of water as stable byproduct and also enable the reaction to occurs at much lower temperature [6]. Moreover, the presence of oxygen reduces the coke formation therefore leading to stable catalytic activity [5], [7]–[9].It worth noting that the catalyst used can obtain oxygen directly from the feed stream without requiring additional re-oxidation.

However, in ODH the selective oxidation of n-butane to C_4 olefins (butenes and 1,3-butadiene) is a challenging issue due to the parallel and consecutive reactions resulting from the rapid reaction of dehydrogenated products with O_2 to form stable combustion

products (CO_x), unstable oxygenates and H_2O [7], [10], [11]. Therefore, the key issue is the development of a catalyst that is able only to activate the C-H bonds of alkane [6].

1.2 Thesis Objectives

The aims of this research are:

1. To prepare a carbide catalytic system for oxidative dehydrogenation of n-butane to 1,3-butadiene
2. To test the influence of various supports on the reactivity and selectivity of the prepared catalyst (Bi-Ni/Support).
3. To develop a kinetic model for the reaction.

These objectives are discussed in details as below:

1.2.1 Synthesis and Characterization of Bismuth and Nickel based catalysts

- Preparation of modified bismuth and nickel oxide based catalysts
- Catalyst characterization (TPR, TPD, XRD, BET…etc)
- Catalyst Evaluation in fixed bed type of reactor with continuous flow system.

1.2.2 Kinetic modelling

The availability of design parameters (activation energy (E), rate constants, etc) is the key to development of any process. The kinetic modelling will involve the following tasks:

- To predict the steps in the rate mechanism using kinetic model.
- To estimate the kinetic parameters in the rate equation.
- To fit the experimental data into a proposed model to validate the model.

CHAPTER 2

LITERATURE REVIEW

2.1 Butadiene

1,3-Butadiene is the simplest conjugated diene that is colorless gas with gasoline like odor under normal conditions, noncorrosive, flammable and toxic hence classified as hazardous chemical [12]**.** Butadiene is produced commercially from steam crackers and also as secondary product in the ethylene and propylene. Moreover, Butadiene is produced by dehydrogenation of normal butane through two steps, initially from normal butane to n-butylene and then butadiene [1].

1,3-Butadiene is used as raw material in a variety of reactions including: polymerization, oxidation reactions, substitution reactions and telomerization reactions. The major use of butadiene is for production of synthetic elastomers which represents three quarters of butadiene consumption, in which 30 % is dedicated to "styrene-butadiene rubber (SBR)", 20 % to polybutadiene, 10 % for "styrene butadiene latex"; and 5 % is dedicated to neoprene, nitrile rubber, and acrylonitrile-butadiene-styrene (ABS). While the balance of butadiene is used for production of nylon and miscellaneous products such as textiles, gloves, carpets and so on [7].

2.1.1 Butadiene's Applications

Actually, there are no consumer uses of 1,3-butadiene, but it is primarily employed as building-block material. For instance, Butadiene is mainly used as monomer for production of synthetic rubbers such as "styrene-butadiene rubber (SBR)", nitrile rubber

such as “acrylonitrile butadiene styrene resins (ABS)” and also used as monomer for preparation of butadiene homoploymer [2]**.** It worth noting that two thirds of Butadiene rubber are consumed for the tires manufacturing while the balance is used for production of high impact polystyrene (HIPS). ABS has wide range of application includes electronics, domestic goods, construction materials and automobiles industry which accounts for the 75% of the global consumption [12]**.** Additionally, many goods are manufactured from rubbers and latexes that made from butadiene, for example: gloves, wetsuit, carpets, waders, gaskets, hoses, seals and paper coatings.

2.2 Butadiene Production Processes

There are three commercial processes for production of Butadiene as summarized below:

- Steam cracking of hydrocarbon feedstocks (LPG, Naphtha ...)
- Catalytic dehydrogenation of n-Butane or Butene (Houdry Catadiene process)
- . Oxidative Dehydrogenation of n-Butene (Oxo-D or O-X-D process).
- Oxidative Dehydrogenation of n-butane.

2.2.1 Steam Cracking Process:

Over 95% of global production of butadiene accounts for the steam cracking process. The process comprises two distinct steps, initially the stream of mixed-C4 -which contains butadiene - is a byproduct in the alkene plant during the cracking of large molecules feedstocks to produce alkenes, then the butadiene is recovered from the mixed-C4 stream through the butadiene recovery unit. The quantity of produced butadiene is primarily dependent on the type of feedstock and how severe the cracking operation is[1], [5]**.**

The hydrocarbon feedstock (light alkanes, naphtha and gas oil) is heated and combined with steam, then fed to pyrolysis furnace operates at temperature range (790–830 ◦C) where it cracks into lighter hydrocarbon among which hydrogen, ethylene, propylene, butadiene and other by-products. After that the pyrolysate (cracking products) is quenched to separate the hydrocarbon products with high boiling point; compressed for removal of C_5 and heavier materials as raw gasoline. Then the remaining products is sent to a number of distillation columns to separate H_2" ethylene, "propylene and other C_2, C_3 components, leaving only C_4 products or crude butadiene [1], [5].

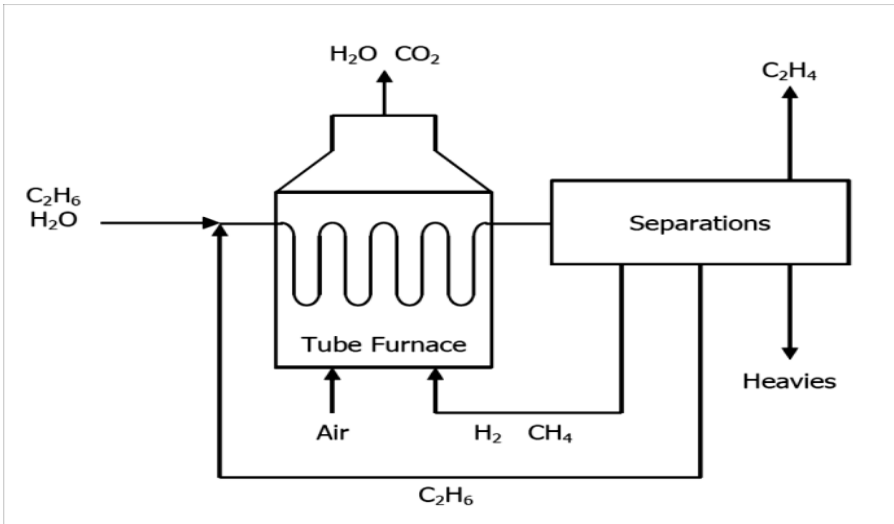

Figure 1 Pyrolysis Furnace (Steam cracking process).

It is well known, that light hydrocarbon feedstock (ethane and propane) produces very low quantity of Butadiene, on the other hand the heavy feedstock (naphtha, gas oils and condensates) results in much greater quantity of butadiene [9]. Table.1 reports a typical yield of steam cracking products from different feedstocks [5]**.**

Table 1 Products yield from steam cracking process for different feedstocks.

Yield (wt%)	Gasous feeds			Liquid feeds	
	Ethane	***Propane***	***Butane***	***Naphtha***	***VGO***
H_2 and Methane	13.0	28.0	24.0	26.0	23.0
Ethene	80.0	45.0	37.0	30.0	25.0
Propene	1.1	14.0	16.4	14.1	14.4
1,3-Butadiene	**1.4**	**2.0**	**2.0**	**4.5**	**5.0**
Mixed Butenes	1.6	1.0	6.4	8.0	6.0
C_5^+	1.6	9.0	12.6	18.5	32.0

2.2.2 Catalytic Dehydrogenation Process

The catalytic dehydrogenation of n-butane is an endothermic process that requires a catalyst. Generally, this process has two steps; initially the normal butane decomposes to butene and then to 1,3-butadiene [1].

The most common process for catalytic dehydrogenation is Houdry Catadiene process, in which the n-butane is dehydrogenated at high temperature (600-680 °C) over CrO_2/Al_2O_3 catalyst which is usually regenerated after few minutes of usage using air to burn off the coke layer, this process is carried out using three of more parallel reactors for the sake continuous operation simulation, Once the catalyst is deactivated in the first reactor due to coke formation ,the feed stream switches to the second reactor. The coke is burnt off in unused reactors and the heat stored for the next operation cycle. The effluent stream from the reactor is quenched, cooled and then compressed before entering the

absorption and stripping column where C_4 products is obtained to be fed to the butadiene recovery unit for purification as shown in Figure.2:

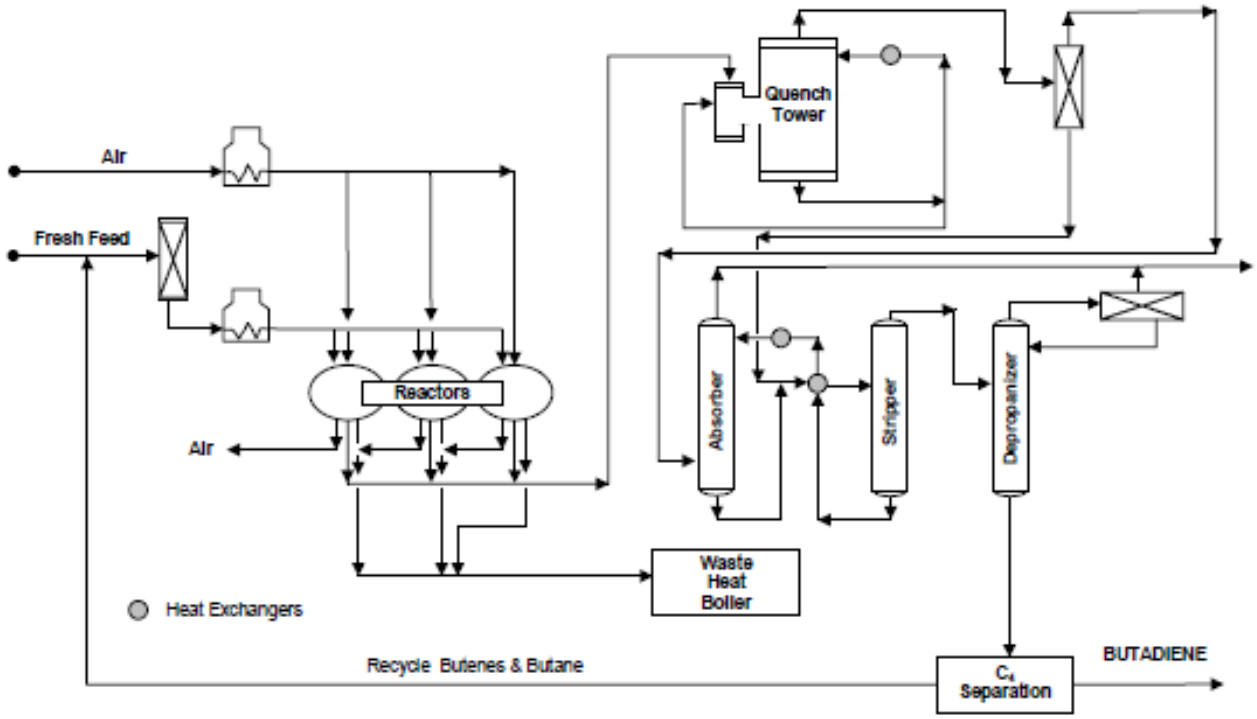

Figure 2 Houdry Catadiene process.

The steam cracking and catalytic dehydrogenation processes share the same drawbacks,

since they are endothermic reactions that require large amount energy and the coke formation which causes catalyst deactivation. Additionally, the catalytic dehydrogenation reaction is thermodynamically limited to high yield of butadiene at low temperature [1], [5].Therefore, the endothermic nature, together with the high temperature required make these processes very energy intensive. Furthermore, the selectivity control is very challenging at this high temperature[5]**.** Therefore, many approaches of research were done to develop a process that overcomes the limitations mentioned above, one of them is dehydrogenation under oxidative conditions either for butene or butane.

2.2.3 Oxidative Dehydrogenation of Butene (Oxo-D Process)

Dehydrogenation of n-butenes in oxidative conditions has replaced many older on-purpose production processes of butadiene. The advantages of using butane as feedstock are: butane is highly reactive and it doesn't require severe operation conditions compared to butane.

In this process, oxygen is used as a co-feedstock, the oxygen acts to displace the equilibrium between butenes and butadiene towards greater production of the diolefins. It removes H_2 by combustion producing water as a byproduct, initiates dehydrogenation by hydrogen abstraction and also ox datively regenerate the catalyst.In general, the n-butenes feed combined with steam and air, then the resulting mixture passed over the catalyst at temperature range 500-600 °C. The butadiene yield and selectivity from this process; can range from 70 - 90 % [2]**.**

2.2.4 Oxidative Dehydrogenation of Alkanes

ODH of alkanes has been suggested as a promising method for olefins and di-olefins production, ODH overcomes the limitations of conventional on-purpose production units such as the thermodynamic limitation on selectivity and activity, side reactions, high temperature requirement and coke deposition [13]**.**Introduction of oxygen to the reactive mixture allows the abstraction of hydrogen and forms H2O as stable byproducts. On the other hand, the presence of steam allows for catalyst activation by removal of coke via gas shift reaction, or serves as heat sink , hence the reaction can proceed in low temperature [14]**.**

It has been generally recognized that the surface acid–base character and the catalyst's redox property to play an important role in the selectivity and catalytic activity for ODH.

Regarding the redox property, the lattice oxygen of the catalyst is involved in oxidation leading to reduction of catalyst surface, then" it is restored to its initial state by adsorption of O_2 from the gas phase" [11].

However, in ODH process, the selective oxidation of n-butane to butadiene is challenging issue due to the parallel and consecutive reactions resulting from the rapids reaction of dehydrogenated products with O2 to form stable combustion products (COx), unstable oxygenates and water. Therefore, the key issue is the development of a catalyst that is able to activate only the C-H bonds of paraffin [6]**.**

Several researchers reported vanadium oxide with different oxides as carriers (Alumina, Silica, Titania, Zirconia, Ceria etc) showing good results for the ODH of lower paraffins. The catalytic performance relies on the type of carrier, catalyst loading and synthesis method [15]. Hakuli et al [16]. investigated different chromia supported catalysts and concluded that alumina and silica-supported chromium oxides were the most effective for the production of lower olefins. Vanadia supported on basic supports not acidic or neutral oxides have been found to be the most selective catalysts for propane ODH as reported by Corma et al [17].Volpe et al [18] concluded from his investigation on "n-butane dehydrogenation using VO_x supported on USY, NaY", γ-Al_2O_3 and α-$A_{l2}O_3$ that VOx/USY has the highest activity and selectivity due to VOx monolayer and its mild acidity. Investigation on the reactivity of vanadia on various supports was conducted by Arena et al [19] and the conclusion drawn was that vanadia was more reactive on amphoteric oxides with TiO_2 having the highest reactivity and that the dispersion and reducibility of the active phase is greatly influenced by the acidic/basic property for the support.

Chromia-Alumina is a dual functional catalyst due to its acidic function obtained from the support and dehydrogenation function due to chromium oxide. Vuurman et al [20] reported that the catalytic dehydrogenation properties of the Chromia-Alumina catalyst are due to surface chromium oxide species and not the bulk chromium oxide phases like CrO_3 or Cr_2O_3. De Rossi et al [21] investigated "propane dehydrogenation on Chromia/Silica and Chromia/Alumina catalysts" and concluded that, the active sites for the dehydrogenation are CrIII and not CrII species and that Chromia supported on zirconia has the highest activity compared to silica and alumina supports. This is because the proper coordination of chromium on the surface sites of zirconia is preserved and the oxygen ion necessary for reduction (H_2 abstraction) is more readily available.

Jibril et al [22] investigated the ODH of iso-butane on chromium oxide-based catalyst, they tested different supports (Al_2O_3, TiO_2, MgO, and SiO_2), different chromium precursors and partially substituting the chromium with some metals (V, Ni, Co, Mo and Bi). They concluded that, chromia supported on alumina has the best performance with chromium nitrate as the best precursor and that partial substitution of chromium by the metals has little or no contribution on the catalyst performance with Nickel addition slightly increasing the selectivity with same conversion.

Ajayi et al [23] studied "n-Butane dehydrogenation over mono and bimetallic MCM-41"(highly dispersed Silica) catalyst under oxygen free atmosphere by varying the weight percent of the metals in the catalyst. They concluded that 1.2Cr2.8V/M-41 has the highest conversion and selectivity toward butene.

2.3 Catalysts for ODH

The catalyst systems studied by several researchers as obtained from literature for ODH of lower alkanes can be grouped into three.

- Catalyst based on alkali and alkali earth metals
- Catalyst based on noble metals
- Catalyst based on oxides of transition metal

2.3.1 Catalyst based on Alkali and Alkali Earth Metals

Catalysts based on Group 1 and 2 metals show good olefin selectivity for ethane and propane, of this catalyst systems the most prominent one is Li/MgO. Although Li/MgO combination shows reasonable activity [24], the catalyst is usually promoted with halogens mainly chlorine. And so halides have high significance towards achievements of good yields resulting from their acidic properties that positively affects dehydrogenation reaction. These catalysts activate ethane at temperature above 600 ^{o}C to produce ethyl radicals that react in the gas phase [25]. Addition of Tin oxide (SnO_2), Lanthanium oxide (La_2O_3), Neodymium oxide (Nd_2O_3), or Dysprosium oxide (Dy_2O_3) further improves the performance of Li/MgO [26]. Ethene yield is up to 77% when Dy_2O_3 is used as a promoter and a remarkable selectivity is achieved when the reaction temperature gets closer to melting point of LiCl [26].

Propene is a best alkene for production through ODH of propane. Ethene can as well be synthesized in large quantity via catalytic dehydrogenation, chemical industries still maintain steam cracking for ethene production.

2.3.2 Catalysts based on Nobel Metals

Catalysts in this group have active species that contains noble metals such as Platinum, Rhodium, Palladium, which are very efficient catalysts for combustion. Paraffins can be converted to alkenes using nobel metal catalysts under specific reaction conditions like reduced contact times and little oxygen supply [4]. At lower temperatures these noble metal catalysts are usually non-selective, however they can be used for selective oxidation at temperature around 1000 ºC, non-oxidative same phase reactions greatly influence the formation of products. The selectivity is enhanced by high alkane-oxygen ratio as well as a higher temperature. This leads to nearly complete conversion of oxygen in a way that non-oxidative conversion of paraffins results like steam reforming together with cracking. The catalyst mainly deactivates due to coking and sintering [27]. Enclosing the active nobel metals in a passive support helps mitigate the deactivation. The over layer of support suppresses the ODH process and prevents sintering of metals with decrease in coke formation for high temperature reactions.

2.3.3 Catalyst based on Transition Metal Oxides

This category of catalyst allows low temperature activation of alkanes relative to group I and II as well as nobel metals. Hence the performance of catalysts for this group is usually better. The ODH reaction of lower paraffins using oxides of metals in the transition series on a support occurs via the mechanism of Mars and Krevelen, in which lattice oxygen in the catalysts is used for oxidizing the paraffin as well as the reoxidation by the gas phase molecular oxygen [23]. Some factors dictate the performance of the catalyst like the redox property, chemical nature of the active oxygen species and the

acid-base character, which in turn depend on the loading and dispersion of the transition metal and the kind of support used [28].

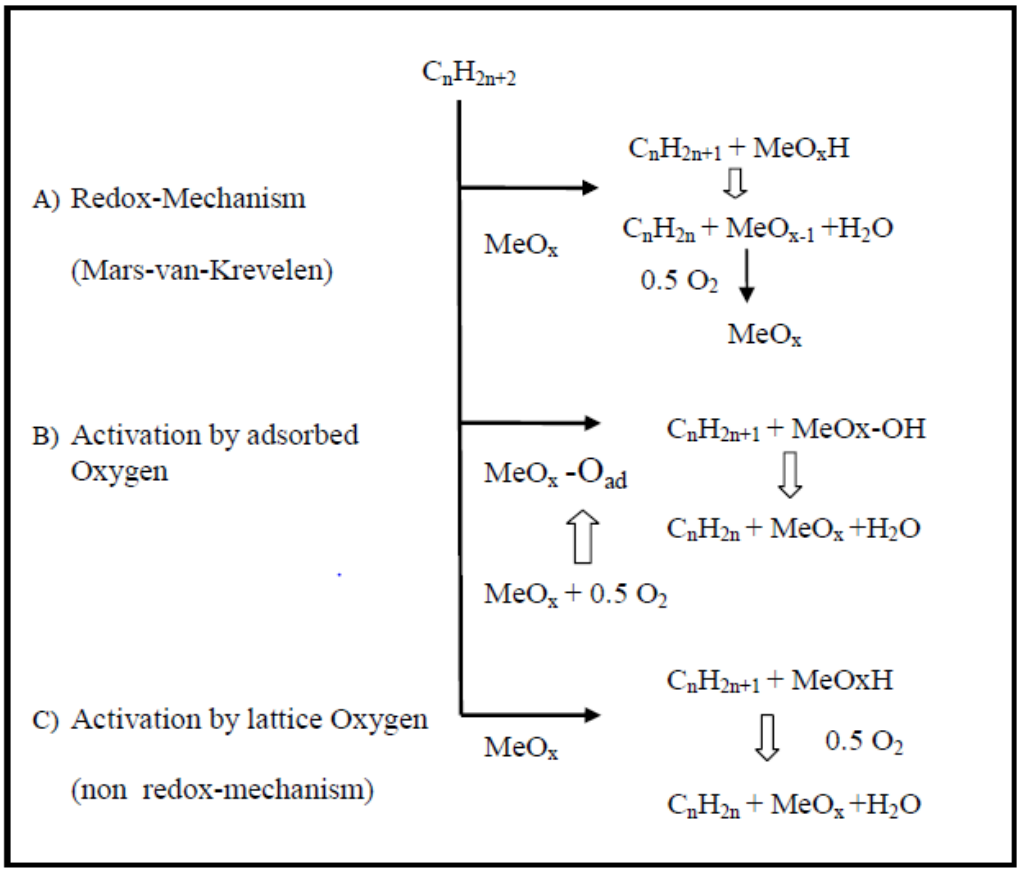

Figure 3: ODH of lower alkanes on transition metal oxides reaction steps [4].

Transition metal oxides have reducible oxygen (surface lattice oxygen) that partake in ODH in the absence of gaseous oxygen. Even though, the active oxygen specie partakes also in other non-selective routes of ODH resulting to CO_x. The two most important systems are the molybdenum-based catalytic system and the vanadia –based catalytic system although from literature the molybdenum systems are less active.

2.4 Reactions Network:

This is a reaction that involves series removal of molecule of hydrogen from normal butane forming 1,3-Butadiene in the presence of oxygen with water as a byproduct. Normal butane is a saturated and highly stable hydrocarbon hence requires high temperature for the activation process, it is slightly different from the ODH of ethylene and propylene because of the presence of two secondary atoms of carbon (-CH_2-) hence it has high chance of undergoing side reactions to yield other products as shown in figure.4

2.5 Reaction Mechanism:

Many literatures, reported that the kinetics of ODH following Mars-van Krevelen redox mechanism where the active species oxygen participates in the ODH reaction by removing molecule of hydrogen from the paraffin thereby forming water as a byproduct which is removed by surface dehydration. The reduced surface is re-oxidized by dissociative chemisorption of oxygen from the gas phase. It has been proposed that O–H group, surface oxygen and oxygen vacancies (reduced sites) are the most abundant reactive intermediates during ODH. The number of catalytically reduced sites on catalyst surface depends mainly on paraffin/oxygen ratio [4].

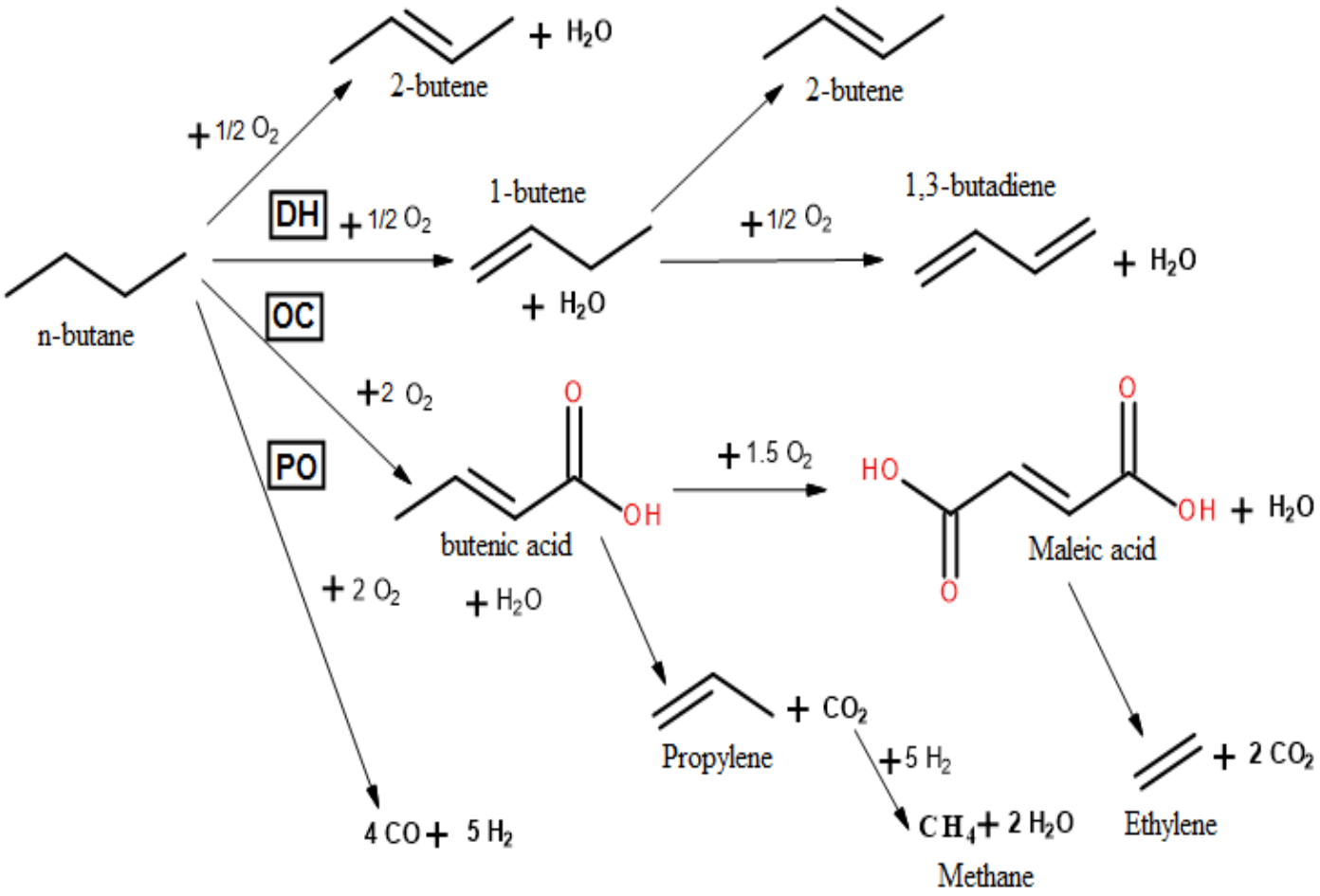

Scheme 1 Selectivity chart from n-butane to butadiene, DH: oxidative dehydrogenation; BD: 1,3-butadiene; OC: oxygenate and cracking formation; PO: partial oxidation reaction. Broken line square inside is stoichiometric oxygen requirement.

2.6 Main Factors Acting in ODH

2.6.1 Surface acid-base character of the catalyst:

Metal oxides consist of redox metal cation (acidic sites) and lattice oxygen anions (basic sites). The acidic-basic properties of the oxide have three main influences on activation of n-butane molecule, on the rates of side reactions and on the adsorption rate of reactants and desorption rate of products.

It is well established [29] that during reaction, the acidic surface favors the acid intermediate desorption. On the other hand, the basic surface favors basic intermediate desorption, which then prevent further combustion of the adsorbed species to form stable combustion products such as CO_2 and water. Therefore, the products with an acidic nature (carboxylic acids) will be formed on acid surface while the products with a basic nature,

(alkenes & di-olefins) in ODH reactions, will be formed on basic surface.

The strength and character of acid/basic sites have a significant role on ODH as they participate in the activation of n-butane as for the first Hydrogen removal.

2.6.2 Electron Transfer Property:

In the redox mechanism, initially the oxygen anion O^{2-} is abstracted to be placed in product while the cation is reduced ($M^{n+} + pe^{-} \rightarrow M^{(n-p)+}$). For instance:

$V^{5+}{}_2O_5 + 2e^{-} \rightarrow V^{4+}{}_2 O_4 + \square$ ($\square$ stands for oxygen vacancy). In the absence of O_2 in the feed, the oxygen vacancies are filled by diffusion of O^{2-} from the gas phase. Generally, the oxygen is added to the hydrocarbon feed to promote re-oxidation because the oxygen diffusion is very slow. The catalyst reduction takes place in the surface as follows:

$O_2 + 4e^- + 2\square_{surf} \rightarrow 2O^{2-}_{surf}$. The property of electron transfer has a key role in the Mars and van Krevelen mechanism.

2.6.3 Nature of Oxygen Species Present on The Catalyst:

It is well known that chemisorbed, weakly bound electrophilic species e.g. O^{2-} , O^- , on the surface of catalyst will result in total combustion of n-butane molecule. The difference in the affinity of the active oxygen specie to bind with paraffins is among the main factors that determines the performance (activity and selectivity) of most metal oxides supported catalysts [29]. A study by Weckhuysen and Keller [30]on vanadium oxide supported catalyst reported that 3 categories of lattice oxygen bonds are associated with the catalysts which are end V=O, intermediate V-O-V and V-O-Carrier bonds each with different binding strength. They concluded that the lattice oxygen from the V-O-Support bond is the one that is involved in the catalytic reduction reaction.

2.6.4 Influence of Support:

Many literatures reported that supported V_2O_5 is a potential catalyst for the ODH of normal butane. “MgO supported vanadium” was found to be selective catalyst for ODH of n-butane.On the other hand, $V/A1_2O_3$ showed high selectivity for ethane for ODH of ethane,but a very low selectivity in -butane ODH. This difference in behavior is ascribed to the acid/base property of the support. Therefore, acidic or basic property of the support controls the catalyst selectivity and reactivity due to their influence on reactants adsorption and product desorption.

2.7 Catalyst Development For n-butane ODH

The literature shows that 1,3-butadiene is produced as co-product for several catalysts used in ODHof n-butane.. Among these catalysts, zinc-chromium-ferrite catalyst [30].

The chromium acts as a promoter that substitutes Fe^{3+} in the octahedral sites which increases the basicity of the lattice oxygen thereby enhancing the selectivities to butadiene and CO2.Vasil'ev and Galich [21]reported that the method of active components deposition on the support strongly determines the performance of "cobalt-molybdenum and magnesium-molybdenum catalyst used in the ODH of normal butane. Catalyst activity increases proportionally to the number of active components which are cobalt, magnesium and molybdenum" especially with a support of low surface area. Vanadia supported on silica gel catalyst [22] was investigated for dehydrogenation of n-butane. The influence of VOx loading and reaction temperature were studied and they concluded that at low VO_x loading and temperature of 590~600 ^oC, n-butane conversion and olefin yield of highest value was obtained.

The effect of vanadia species in VO_x/Al_2O_3 for n-butane dehydrogenation by varying the vanadium loadings was investigated by McGregor et al [23]. The catalysts were characterized using FTIR and solid state NMR and concluded from their findings that a strong relationship exist between the surface species of VO_x and the performance of the catalyst with high activity and low selectivity for isolated VO_x species and polymeric VO_x species having greater selectivity to the targeted olefins.

Lee et al [24] investigated oxygen mobility influence together with oxygen capacity of Mg3(VO4)2 supported with different oxides (Al_2O_3, ZrO_2, MgO, CeO_2) for ODH of n-butane. Their experimental findings shows that at the initial stage of the reaction $Mg_3(VO_4)_2$/MgO is the most active catalyst and $Mg_3(VO_4)_2$/ Al_2O_3 the least active. The activity decreases with time for the MgO catalyst while $Mg_3(VO_4)_2/ZrO_2$ showed stable

catalytic activity, hence the conclusion that oxygen mobility and oxygen capacity directly affects the stability of the catalyst activity and the initial catalytic activity respectively.

Jermy et al [28] investigated the catalytic ODH of normal butane to butadiene using Bi-Ni-O/γ-Alumina and reported from their experimental findings that the support itself is selective for the ODH of n-butane to butenes and partial oxidation to CO, the dispersion of NiO on the support reduces the partial oxidation selectivity and enhanced butadiene selectivity. Addition of bismuth to the catalyst was confirmed to yield higher butadiene selectivity due to improved dispersion of NiO and the efficient redox cycle of the resulting catalyst.

Kwon Lee et al [25] in a similar study investigated the ODH of normal butane to normal butene and 1,3-butadiene over $Mg_3(VO_4)_2$/MgO-ZrO_2 catalyst with varying Mg:Zr in the support. The support was prepared using gel-oxalate co-precipitation method and the catalyst by wet impregnation method and was characterized using XRD, XPS and ICP-AES techniques. They concluded that the catalyst with Mg:Zr of 4:1 has the highest activity and selectivity due to its highest oxygen capacity and acidity as confirmed by TPRO and TPD respectively. Xu et al [26] investigated the catalytic ODH of n-butane over V2O5/MO-Al2O3 (M= Alkaline earth metals: Mg, Ca, Ba, Sr) with varying V_2O_5 loading. The catalyst characterization were performed by N2 adsorption, XRD, FTIR, H_2-TPR and Raman spectra and the results showed that only MgO modified Alumina produce a catalyst with high activity and selectivity while that of Ca, Ba and Sr showed low activity due to the formation of orthovanadate phase which seldom undergoes reduction. The high activity of the MgO modified Alumina is due to the good dispersion

of VO_x species due to increased surface area of the support and the existence of crystalline phase of MgO.

2.8 NiO Based Catalyst For ODH On n-Butane:

Nickel oxide is a relatively less expensive oxide that has been reported to activate short chain alkanes (C_2-C_4) in the presence of molecular oxygen with resulting high activity and at low reaction temperatures. The products obtained however are mainly oxidation products (CO and CO_2) with little dehydrogenation products. The nature of Ni species and the acidity/basicity of the catalyst are the two factors that influence its performance as a catalyst. NiO has been reported to have improved performance in its activity and selectivity when supported or promoted on metal oxides. This promotion reduces the selectivity of oxidation products and enhanced that of dehydrogenation [27].

Jermy et al [28] reported that NiO when promoted with Bismuth oxide results in an improved performance, this is due to the participation of Bi_2O_3 as oxygen mobile oxides which is critical in the formation of electrically active grain boundaries in the NiO.

CHAPTER 3

EXPERIMENTAL SETUP AND PROCEDURES

3.1 Experimental Setup

3.1.1 Fixed Bed Tubular Reactor System

The reaction system is a complete reaction microsystem for the evaluation of the catalyst while analyzing the data in continuous flow process. The performance of the catalysts is examined using a fixed bed type of reactor with continuous flow system (BELCAT). It comprises a quartz tubular reactor, placed inside stainless steel furnace which passes through the reactor furnace thermo well wall. The catalyst sample (500-850 microns) is placed into the quartz reaction tube (length of heating zone =18 cm, inner diameter = 8

mm). The catalyst bed temperature is monitored with the help of thermocouple, which inserted into thermocouple well

The n-butane and oxygen are mixed to create a non-fluctuating homogeneous stream which is then sent to the reactor. Before sending the feed to the system its flow is controlled with high pressure metering valves. The effluent stream from the reaction system is transferred to a customer-supplied gas chromatograph through a heated transfer line. Two adjustable PID controllers are part of the system control; they are used to control the temperature of the reactor and the oven.

3.1.2 Gas Chromatographic (GC) System

The products and reactants are analyzed with the help of an Agilent 7890N gas chromatograph. The GC consists of FID (N_2 carrier) and GC-GasPro capillary column (length= 600 cm, internal diameter= 0.032 cm) for analyzing the hydrocarbons and oxygenates. The thermal conductivity detector (TCD), Shin Carbon 80/100 mesh SS Column (Helium as a carrier gas) and MS5A 60/80 mesh SS Column (Argon as a carrier gas) were also attached with the GC system for detection of gases including CO, CO2, O2, N2 and H2. The effluents were identified by comparing with authentic samples. The conversion and products selectivity are determined on the basis of carbon balance

3.1.3 Gas Chromatographic (GC) System

The GC Calibration was done to determine the distribution of the reaction products. The retention times of all compounds of interest in this work were determined by analyzing pure samples of each of the compounds in the GC in turns. Table 2 shows the different hydrocarbons and their corresponding retention times and Table 3 shows the retention

times of CO, O_2, N_2 and H_2. These retention times were used to identify each component of the reaction products.

Table 2 Retention times for hydrocarbon components.

Compounds	Retention time (min)
Methane	2.067
Ethane	2.319
Ethylene	2.575
Propane	3.322
Propylene	4.575
Iso-Butane	5.932
n-Butane	6.210
1-Butene	8.910
trans-2-butene	8.537
cis-2-butene	9.745
1,3-butadiene	12.729

Table 3 Retention times for non-hydrocarbon components

Compounds	Retention time (min)
Oxygen	4.839
Nitrogen	5.469
Carbon monoxide	6.99
Hydrogen	1.05

3.2 Experimental Procedure

This section details the procedure to be followed from catalyst preparation, characterization and finally catalyst testing:

3.2.1 Catalyst Preparation

Various Supports material such as TiC, SiC, ZSM5 (with different Si/Al ratio) and Silicalite were used. All supports are commercial products with exception of Silicalite. The Silicalite support was prepared following the procedure reported in [40].

Bi–Ni oxide based catalysts were prepared using co-impregnation technique, using "nickel nitrate hexahydrate (99% Fisher-Scientific) and bismuth nitrate pentahydrate (98 %, Fluka-Garantie)" as precursors for the metals. For synthesizing 30 wt.% Bi-20 wt.% Ni / TiC catalyst, 0.99 of "nickel nitrate hexahydrate was dissolved in 160 ml of distilled water, then 1.392 g of bismuth nitrate pentahydrate" was successfully added to the mixture while stirring at 55 ºC. 2 g of TiC support was added and thoroughly stirred for dissolution. Then, the resultant suspension was left overnight for impregnation. After drying the suspension for 3 h at 120 ºC, the resulting powder was pressed into pellets form, crushed to break up the crumbs and then sieved into 500-850 mesh granules. The binary metal oxides catalysts with different support (SiC and Silicalite…etc) were synthesized in a similar manner. The catalysts used in this research were shown in Table 4.

For catalytic evaluation and characterization, the as-prepared catalyst was calcined using two step calcination method, where the catalyst is heated to a temperature of 350 °C at rate of 10 °C per minute and held for 1 hour after which it was raised again at rate of 15 °C per minute to temperature of 590 °C and kept for 2 hours under flowing nitrogen.

Table 4 Controlling factors of catalysts for Oxidative dehydrogenation of n-butane to butadiene

Main Item	**Sub Item**		**Species/Content (wt %)**
Metal Species		BNFe	5Co 5Fe 10Ni30Bi/TiC
		BNCo	10Co 10Ni 30Bi/TiC
Support	**Zeolite**	BNZ 1500	20Ni30Bi/ZSM-5(Si/Al =1500)
		BNZ 500	20Ni30Bi/ZSM-5(Si/Al =500)
		BNZ 280	20Ni30Bi/ZSM-5(Si/Al =280)
		BNZ 80	20Ni30Bi/ZSM-5(Si/Al =80)
		BNZ 23	20Ni30Bi/ZSM-5(Si/Al =23)
		BNZ -CS	20Ni30Bi/ZSM5-280 (Core Shell)

	Carbide	BNW	20Ni30Bi/WC
		BNT	20Ni30Bi/TiC
		BNS	20Ni30Bi/SiC
	Silicalite	SJC25	20Ni 30Bi/Silicalite
		BNS-1	10Ni20Bi/Silicalite
		BNS-2	20Ni 10Bi/Silicalite
		BNS-3	60Bi 20Ni/Silicalite
	TiC	BNT-1	10Ni20Bi/TiC
		BNT-2	20Ni 10Bi/TiC
		BNT-3	60Bi 20Ni/ TiC
		BNT-X	25Ni37.5Bi/TiC

3.2.2 Catalyst Characterization

Surface area and pore structure of sample were measured by N_2 adsorption measurements at 77 °k" using Micrometrics ASAP 2020 apparatus (Norcross GA). All samples (ca.0.05 g) were outgassed at 240 ^{o}C under flowing nitrogen for 3 h prior to measurements. The surface area and pore size were obtained by employing Barrett–Joyner–Halenda (BJH) method.

The powder X-ray diffraction was carried out on Rigaku Miniflex II instrument employing Cu Kα radiation source (wave length = 1.5406 Å). The working voltage and current of the apparatus were 40 kV and 30 mA, respectively. XRD patterns were

recorded over an angular range (2Θ) of 5-90^{o} at scanning rate of 2^{o}/min and step size of 0.02^{o}.

a BELCAT-A-200 chemisorption apparatus was used for temperature programmed reduction (TPR) and temperature programmed desorption (TPD). The equipment consists of U-shaped quartz tube having furnace, and a pair of mass spectrometer and thermal conductivity detector (TCD). Gas pulses with standard volume were injected into He background flow to establish the linearity of the TCD response. For each H_2-TPR analysis, the sample (ca.100 mg) was placed into U-shaped quartz tube and preheated at 300 ºC for 3 h in a He flow and then cooled down to the room temperature. Then the flow was switched to a gas mixture of Ar/H_2 (95/5 vol%) with constant flow rate of 50 cm^3/min, then the sample was heated at rate of 20 ^{o}C/min to 900 ºC. The amount of H_2 consumed was measured by TCD and CuO was utilized as reference for calibrating the hydrogen consumption.

Carbon dioxide and ammonia temperature programmed desorption (CO_2 and NH_3-TPD) were conducted in the same BELCAT-A-200 instrument for measuring the basicity and acidity respectively. Sample (ca.100 mg) was preheated at 500 ^{o}C in helium flow (50 ml min^{-1}) and maintained for 1 h before cooling down to 100 ^{o}C. Then, the sample was exposed to He/CO_2 mixture (He/NH_3 mixture for NH_3-TPD) having a volume ratio of (95/5 vol%) for ½ h. Then, sample was purged using He stream at 100 ^{o}C for 1 h to remove physisorbed CO_2 (NH_3) from the sample's surface. Sample was then heated using the same He flow at a heating rate of 10 ^{o}C/min to 600 ^{o}C, while measuring the evolved CO_2 (NH_3) using TCD or mass spectrometer.

3.2.3 Catalytic Evaluation

The performance of the as-prepared catalysts was examined using a fixed bed type of reactor with continuous flow system (BELCAT). Typically",300 mg of the as-synthesized catalyst was placed into the quartz reaction tube. Prior to the reaction, the as-synthesized sample of the catalyst was pretreated at high temperature under flowing nitrogen. Afterwhich the catalyst was cooled down to the reaction temperature using nitrogen. Then, catalytic tests were conducted at reaction temperature of (400,450 and 500 ^{o}C) and different reactant feed ratio (O_2: n-C_4H_{10} = 1.0 ,2.0 and 4.0 mol mol^{-1}).

Taking into account the exothermic nature of oxy-dehydrogenation reaction, the catalyst bed temperature was monitored with the help of thermocouple, which inserted into thermocouple well. The products and reactants were analyzed with the help of an Agilent 7890N gas chromatograph.

CHAPTER 4

RESULTS AND DISCUSSION

4.1 Catalytic Evaluation

4.1.1 Influence of different supports:

There is a general agreement that supports have significant effects on the catalytic performance. In this work, the influence of different support species on the catalyst performance for ODH of n-butane to butenes and 1,3-butadiene was examined in the reaction conditions of O_2/n-C_4H_{10} = 2 and 450 ºC as shown in Table 5. The major

reaction products were obtained from dehydrogenation reaction (DH: 1-butene, cis-2-butene, trans-2-butene, 1,3-butadiene), oxygenate formation and cracking (OC: carboxylic acids & lighter alkenes mainly C_2H_4 & C_3H_6) and partial oxidation (PO: CO), whereas negligible amounts of methane, ethane, propane and carbon dioxide were detected by the GC analysis. The reaction pathways including the side reactions (Oxygenate & cracking, partial oxidation) is shown in Scheme 1. Under the reaction conditions employed in the present contribution, the pristine supports were found to be inactive for ODH of n-butane. The supported catalysts exhibited different degrees of selectivity towards the desired products due to the difference in supports species.

Table 5 Catalytic performance for 30 wt%Bi-20 wt%Ni/support (Support: None, TiC, SiC & Silicalite) at 450 ºC and O_2/n-C_4H_{10} = 2 for ODH of n-butane.

Catalyst	Bi-Ni	Bi-Ni/TiC	Bi-Ni/SiC	Bi-Ni/Silicalite
n-C_4H_{10} Conversion [%]	3.8	16.6	15.1	12.4
Selectivity[*1] [C%]				
DH	39.9	83.7	87.3	71.0
C_4H_8[*2]	36	33	60.2	53
BD	3.9	50.7	27.1	18.0
OC	55.4	12.3	10.6	24.0
PO	4.7	4.0	2.1	5.0
BD yield	0.1	8.4	4.1	2.2
DH yield	1.5	13.9	13.2	8.8

[*1] DH: dehydrogenation, OC: oxygenate and the cracked, BD: 1,3-butadiene, PO: partial oxidation.

[*2] C_4H_8: includes 1-C_4H_8, trans-2-C_4H_8, cis-2-C_4H_8

As evident from Table.5, the unsupported Bi-Ni catalyst presented the poorest catalytic activity compared to supported catalysts, which can be ascribed to the smaller surface

area. The catalytic activities of Bi-Ni catalysts on various supports followed the order: Bi-Ni/TiC > Bi-Ni/SiC > Bi-Ni/Silicalite. As regards the unsupported Bi-Ni catalyst, the lowest dehydrogenation selectivity was observed. Obviously, the predominant reaction products over Bi-Ni/SiC and Bi-Ni/TiC were butenes and butadiene, which indicates that the parallel side reactions hardly take place on these catalysts. Particularly, Bi-Ni/SiC exhibited high dehydrogenation selectivity, approximately over twofold greater than the unsupported catalyst. A similar dehydrogenation selectivity was observed for TiC-supported catalyst, while the formation of 1,3-butadiene remained at 50.7% and greater compared to butenes (33%). Compared to SiC and TiC-supported catalyst, Bi-Ni/Silicalite catalyst showed slightly lower dehydrogenation selectivity (71%). As expected, the highest oxygenate and cracking (OC) selectivity was observed over unsupported Bi-Ni catalyst. Whereas, the selectivity towards side reaction (PO & OC) products decreased significantly when TiC and SiC are chosen as supports. The partial oxidation selectivity remained at low level for all catalysts, pointing out that none of these catalysts in favor of that reaction pathway. It can be inferred from the aforementioned findings, the occurrence of parallel side reactions (especially cracking one) is highly affected by support type to some extent.

Concerning the ZSM5 supported catalysts, the highest conversion was observed over ZSM5 (Si/Al = 1500) supported catalyst, whereas ZSM5 with Si/Al= 80 and 500 (hereafter named ZSM5-80 & ZSM5-500) recorded the lowest conversion of 8% and 7.7% respectively as shown in Table 6 & 7. As regards the DH selectivity, ZSM5-280 has the highest followed by ZSM5-1500 while ZSM5-180 has the least DH selectivity, while the opposite trend was observed in OC selectivity, this shows that ZSM5-180 support

serve as a more selective catalyst for cracking. The order of the BD selectivity as the catalyst support is ZSM5-280 > ZSM5-1500 > ZSM5-80 > ZSM5-23 > ZSM5-280 (Core shell) > ZSM5-500 > ZSM5-180. The PO selectivity remained at low levels for supported catalysts investigated with exception of ZSM5-80 and ZSM5-23 supported catalysts. On the other hand, tungsten carbide (WC) supported catalyst showed good dehydrogenation and butadiene selectivity but have weak activity, this is due to their inability to activate n-butane.

Table 6: Catalytic performance for 30 wt%Bi-20 wt%Ni/supported on ZSM5(Si/Al=1500, 280, 80 & 23). Reaction conditions: 450 °C and O_2/n-C_4H_{10} = 2.

Catalyst supports	**ZSM5-1500**	**ZSM5-280**	**ZSM5-80**	**ZSM5-23**
n-C_4H_{10} conversion [%]	22.7	13.6	8.0	13.1
Selectivity*[1] [C%]				
DH	**35.2**	**61.1**	**25.4**	**21.3**
1-C_4H_8	6.5	11.7	2.4	2.2
BD	**17.2**	**20.3**	**16.9**	**14.0**
OC	45.0	31.7	36.1	42.7
PO	19.8	7.2	38.6	36.0
BD/DH %	48.8	33.2	66.7	65.9
(1-C_4H_8 + BD)/DH %*[2]	67.4	52.3	76.2	76.4
BD/(1-C_4H_8 + BD) %*[3]	72.4	63.4	87.5	86.3

BD yield	3.9	2.8	1.4	1.8

[1] DH: dehydrogenation, BD: butadiene, OC: oxygenate and the cracked, PO: partial oxidation,[2]selectivity at 1st step dehydrogenation, *[3] selectivity at 2nd step dehydrogenation.

Table 7 Catalytic performance for 30 wt%.Bi-20wt%.Ni/supported on WC and ZSM5(Si/Al=500, 280 core shell, 80 & 23). Reaction conditions: 450 ºC and O_2/n-C_4H_{10} = 2.

Catalyst supports	**ZSM5-500**	**ZSM5-280 (Core Shell)**	**ZSM5-180**	**WC**
n-C_4H_{10} conversion [%]	7.7	11.5	17.2	9.5
Selectivity*[1] [C%]				
DH	**34.4**	**32.3**	**5.7**	**90.2**
1-C_4H_8	7.9	6.9	1.4	28.2
BD	**2.0**	**8.0**	**0.0**	**30.6**
OC	54.5	55.7	86.9	5.8
PO	11.1	12.1	7.4	4.0
BD/DH %	5.9	24.9	0.0	34.0
(1-C_4H_8 + BD)/DH %*[2]	28.9	46.1	25.0	65.2
BD/(1-C_4H_8 + BD) %*[3]	20.5	53.9	0.0	52.0
BD yield	0.2	0.9	0.0	2.9

In Table 6 & 7, selectivity parameters inside dehydrogenation for selective conversion from n-butane to butadiene through 1-butene intermediate are also shown as (1-C_4H_8 + BD)/DH: selectivity at 1st step dehydrogenation, BD/(1-C_4H_8 + BD): selectivity at 2nd step dehydrogenation, and BD/DH: two step total selectivity, = (1-C_4H_8 + BD)/DH x BD/(1-C_4H_8 + BD), based on the concept for selective conversion from n-butane to butadiene thorough 1-butene intermediate. In Table 6, the values of the selectivity at 1st step dehydrogenation: (1-C_4H_8 + BD)/DH are similarly around 70% except for ZSM5-280, whereas, in Table 7 the value varies from 25% with ZSM5-180 to 65% for WC support.

The ZSM5-80 showed the highest selectivity at 2nd step dehydrogenation: BD/(1-C_4H_8 + BD), followed by ZSM5-23 and ZSM5-1500. The high selectivity at 2nd step dehydrogenation over ZSM5-80 indicates that, this support has a very high tendency of enhancing H2 abstraction from 1-butene intermediate. From the results, ZSM5-80 showed the highest value of the two step total selectivity: BD/DH (66.7%). In conclusion, Ni-Bi-O metal oxides cannot perform efficiently without the support as catalyst for the ODH of n-butane to butadiene.

4.1.2 Influence of reaction conditions

4.1.2.1 O_2/n-C_4H_{10} molar ratio

The influence of oxygen to n-butane ratio and temperature on the reaction pathways was explored over different supported catalysts. The oxygen to n-butane ratio is viewed to be an essential parameter influencing the catalytic performance of catalysts. As shown earlier, Bi-Ni/TiC has the highest yield of dehydrogenated products (butenes &

butadiene) among all catalysts, so we focused too much on the influence of reaction conditions on the said catalyst.

As regards Bi-Ni/TiC catalyst, the butane conversion and product distributions are given as function of O_2/n-C_4H_{10} ratio in Table 8. The rate of butane conversion increased linearly with an increase of O_2/n-C_4H_{10} ratio from 1 to 4. As shown in Table 8, the main products are butenes and 1,3-butadiene (BD), the dehydrogenation selectivity to butenes decreased with an increase in oxygen content, while butadiene selectivity rose to the maximum of 51.1% at O_2/n-C_4H_{10} ratio of 2 and then declined to 46.3% at O_2/n-C_4H_{10} ratio of 4. However, the oxygenate and cracking selectivity rose gradually from 1.7% at molar ratio of 1 to 11.1% at ratio of 4. A similar trend was observed for partial oxidation selectivity, this result is in agreement with previous studies [27], [41], [42], which stated that the oxidation reactions resulting in partial oxidation formation are strongly affected by oxygen amount. As shown in Table 8, the lower levels of oxygen hinder the oxidation of n-butane to CO_x and promote the selective oxidation to dehydrogenated products. Obviously, the O_2/n-C_4H_{10} ratio of 2 appears to be the best trade-off between high conversion and satisfactory dehydrogenation selectivity.

Table 8 Influence of O_2/n-C_4H_{10} ratio on catalytic performance. Catalyst:30 wt%Bi-20 wt%Ni /TiC, 400 °C.

O_2/C_4H_{10} ratio	**1**	**2**	**4**
n-C_4H_{10} conversion [%]	8.1	11.5	17.4
Selectivity*[1] [C%]			
DH	**93.8**	**89.0**	**82.5**
1-C_4H_8	13.6	12.1	14.7
BD	**47.5**	**51.1**	**46.3**

OC	1.7	5.7	11.1
PO	4.5	5.3	6.4
BD/DH %	50.7	57.4	56.2
(1-C_4H_8 + BD)/DH %*[2]	65.2	71.1	74.0
BD/(1-C_4H_8 + BD) %*[3]	77.7	80.8	75.9
BD yield	3.8	5.9	8.1

Table 9 Influence of O_2/n-C_4H_{10} ratio on catalytic performance. Catalyst:30 wt%Bi-20 wt%Ni /SiC, 400 °C.

O_2/C_4H_{10} ratio	**1**	**2**	**4**
n-C_4H_{10} conversion [%]	10.2	9.6	11.8
Selectivity*[1] [C%]			
DH	**89.9**	**88.6**	**88.4**
1-C_4H_8	37.6	44.3	36.2
BD	**26.9**	**14.8**	**10.6**
OC	10.1	9.4	6.9
PO	0.0	1.9	4.7
BD/DH %	30.0	16.7	30.5
(1-C_4H_8 + BD)/DH %*[2]	71.8	66.7	71.4
BD/(1-C_4H_8 + BD) %*[3]	41.8	25.0	42.7
BD yield	2.7	1.4	1.25

In case of Bi-Ni/SiC, the n-butane conversion almost remained unchanged when the O_2/C_4H_{10} ratio increased from 1 to 4. A similar trend was observed for DH selectivity, while BD selectivity decreased with doubling the feed ratio. Regarding OC selectivity, a decreasing trend was noticed with an increase of O_2/C_4H_{10} ratio. Whereas an opposite trend was seen for PO selectivity, pointing out that, the presence of excess oxygen leads to partial oxidation of butane feed.

Table 10: Influence of O_2/n-C_4H_{10} ratio on catalytic performance. Catalyst:30 wt%Bi-20 wt%Ni /Silicalite, 400 °C.

O_2/C_4H_{10} ratio	**1**	**2**	**4**
n-C_4H_{10} conversion [%]	9.9	9.5	10.2
Selectivity*[1] [C%]			
DH	**78.4**	**72.4**	**61.0**
1-C_4H_8	34.4	31.4	26.5
BD	**21.3**	**19.2**	**15.6**
OC	20.4	23.7	27.4
PO	1.2	3.9	11.6
BD/DH %	27.2	26.5	25.6
(1-C_4H_8 + BD)/DH %*[2]	71.1	69.9	69.0
BD/(1-C_4H_8 + BD) %*[3]	38.2	37.9	37.1
BD yield	2.1	1.8	1.6

Concerning Bi-Ni/Silicalite, the butane conversion maintained stability at around 10% when the O_2/C_4H_{10} ratio increased from 1 to 4. The DH and BD selectivity showed a diminishing trend. Whereas the PO and OC selectivity increased from 20.4% and 1.2% at O_2/C_4H_{10} ratio=1to 27.4% and 11.6% at O_2/C_4H_{10} ratio=4 respectively.

Table 11 Influence of $O_2/n\text{-}C_4H_{10}$ ratio on catalytic performance. Catalyst: 5 wt%Co-5 wt%Fe- 30 wt%Bi-10 wt%Ni /TiC, 400 °C.

O_2/C_4H_{10} ratio	**1**	**2**	**4**
n-C_4H_{10} conversion [%]	4.0	7.2	11.9
Selectivity*[1] [C%]			
DH	**97.5**	**89.2**	**72.1**
1-C_4H_8	14.6	12.0	19.8
BD	**45.4**	**48.6**	**26.4**
OC	2.5	9.1	26.9
PO	0.0	1.1	1.7
BD/DH %	46.6	54.5	36.7
(1-C_4H_8 + BD)/DH %*[2]	61.6	67.9	64.2
BD/(1-C_4H_8 + BD) %*[3]	75.6	80.2	57.1
BD yield	1.8	3.5	3.1

As regards Co-Fe-Ni-Bi/TiC, the butane conversion increased from 4% to 11.9% when the feed ratio increased from 1 to 4 mol/mol. The BD selectivity reached the maximum of 48.6% at O_2/C_4H_{10}=2, then decreased to 26.4% at feed ratio of 4 mol/mol. The DH selectivity exhibited a decreasing trend at high O_2/C_4H_{10}, indicating the dehydrogenation reaction is favorable only at low O_2/C_4H_{10}. The cracking reaction is favorable at high O_2/C_4H_{10} since the OC selectivity increased considerably with an increase of feed ratio. The PO selectivity remained at low levels with slight increase.

Table 12 Influence of O_2/n-C_4H_{10} ratio on catalytic performance. Catalyst: 10 wt%Co- 30 wt%Bi-10 wt%Ni /TiC, 400 °C.

O_2/C_4H_{10} ratio	**1**	**2**	**4**
n-C_4H_{10} conversion [%]	6.0	11.6	22.7
Selectivity*[1] [C%]			
DH	**96.7**	**84.5**	**51.1**
1-C_4H_8	16.1	13.7	9.3
BD	**41.8**	**43.5**	**26.8**
OC	3.3	15.5	48.6
PO	0.0	0.0	0.3
BD/DH %	43.3	51.5	52.4
(1-C_4H_8 + BD)/DH %*[2]	59.9	67.7	70.7
BD/(1-C_4H_8 + BD) %*[3]	72.3	76.1	74.2
BD yield	2.5	5.1	6.1

In case of 10Co-30 Bi-10 Ni /TiC, the dehydrogenation reaction dominates at low O_2/C_4H_{10} ratio, then a significant decrease in DH selectivity was observed when the feed ratio increased from 1 to 4. The BD selectivity recorded the maximum value of 43.5% at feed ratio of 2, then dropped to 26.8% at feed ratio of 4. The selectivity towards the oxygenate and cracking products showed an increasing trend with an increase of O_2/C_4H_{10}. The partial oxidation products weren't observed at low feed ratio.

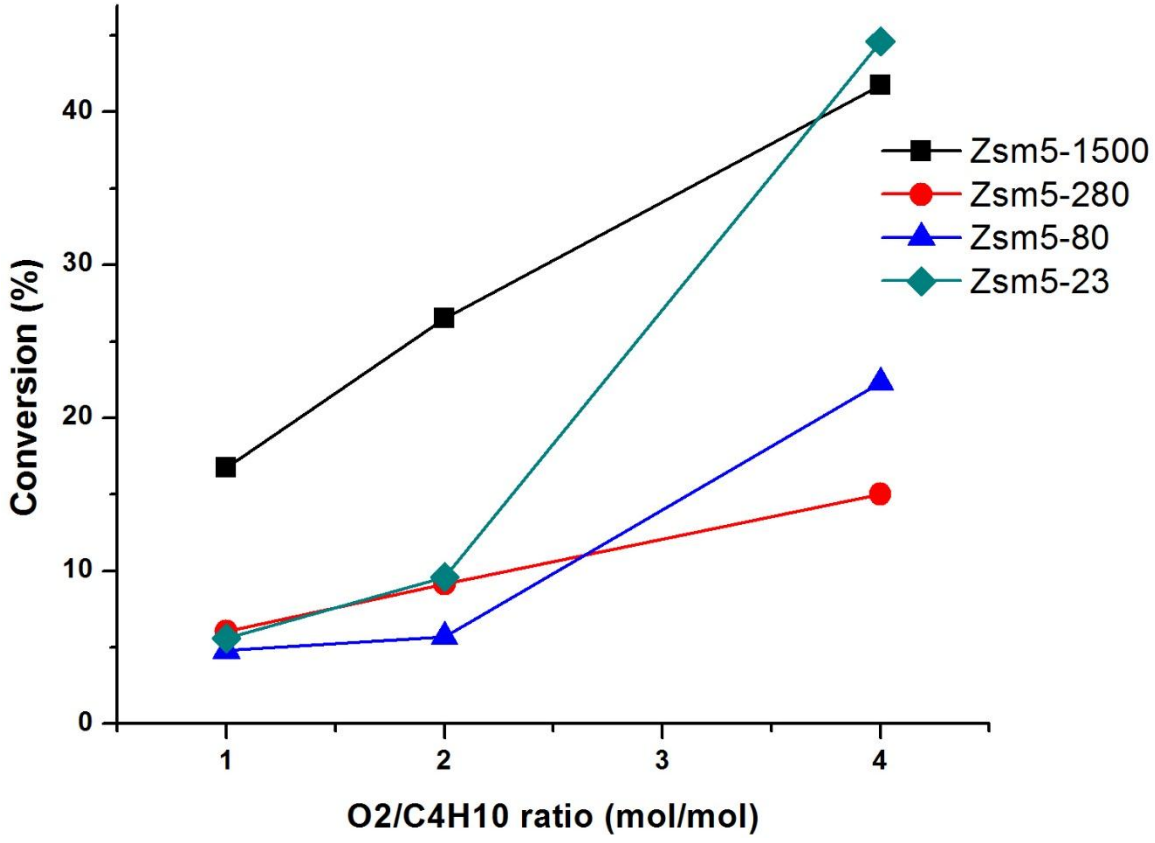

Figure 4 Influence of O2/n-C4H10 ratio on butane conversion. Catalyst: 30 wt%Bi-20 wt%Ni supported on ZSM5 with Si/Al ratio of 23,80, 280 and 1500. Reaction Temperature 400 °C.

The butane conversion for bimetallic 30% Bi-20% Ni catalyst supported on ZSM5 (with different Si/Al ratio) was depicted in Fig 4. The ZSM5 supports with lower Si/Al ratio i.e. ZSM5-23 and ZSM5-80 grew in a second order curve with an increase of $O_2/n\text{-}C_4H_{10}$. Whereas, ZSM5-1500 and ZSM5-280 increased not proportionally but linearly with

oxygen to butane ratio. The highest conversion was recorded by ZSM5-23 supported catalyst followed by ZSM5-1500, while the poorest conversion was achieved over ZSM5-280.

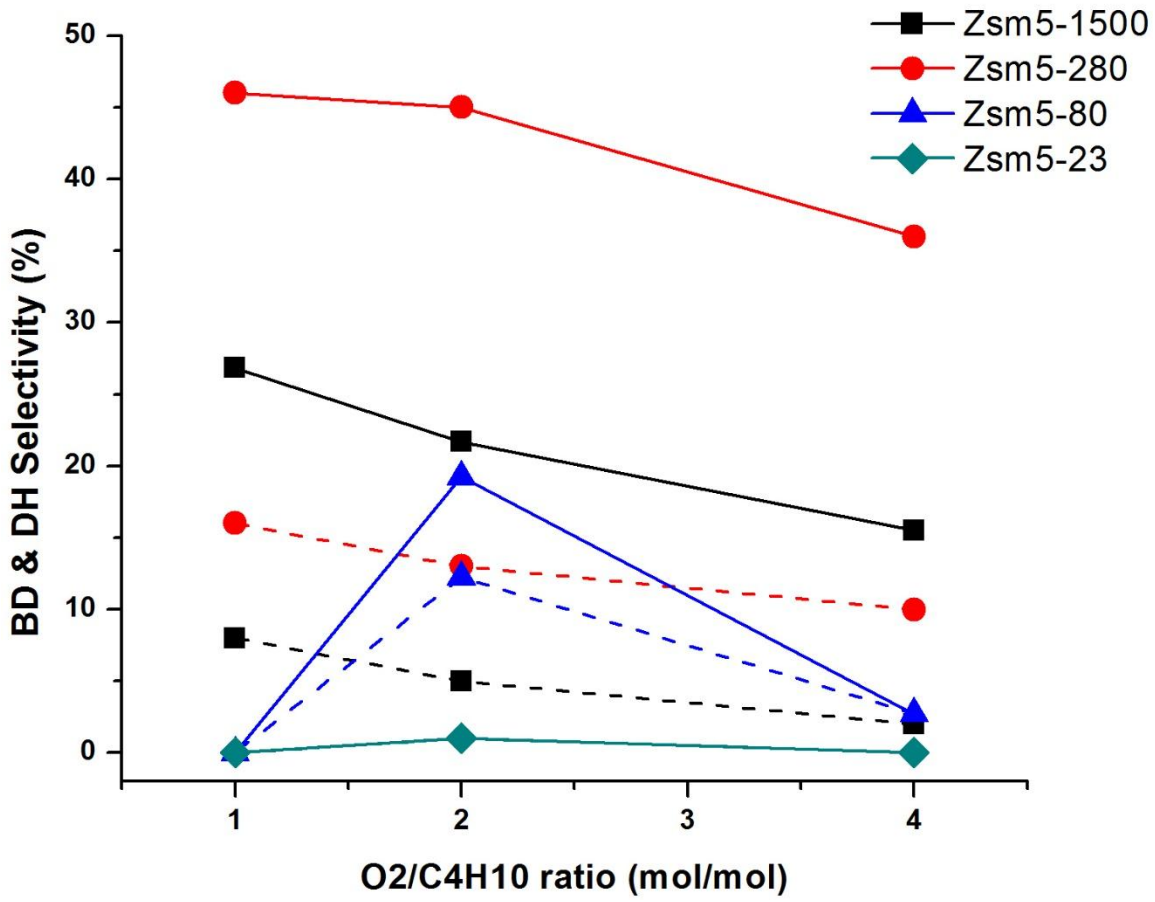

Figure 5 Influence of O_2/n-C_4H_{10} ratio on Dehydrogenation (DH) and Butadiene (BD) selectivity represented by (__) and (- - - -) respectively. Catalyst: 30 wt%Bi-20 wt%Ni supported on ZSM5 with Si/Al ratio of 23,80, 280 and 1500. Reaction Temperature 400 °C

Fig 5 presents the effect of O_2/n-C_4H_{10} on Dehydrogenation and Butadiene selectivity. Both BD and DH selectivity showed a diminishing trend with an increase of O_2/n-C_4H_{10} over ZSM5-1500 and ZSM5-280 supported catalysts due to dominance of partial oxidation reaction at high O_2/n-C_4H_{10} ratio over zeolite catalysts. ZSM5-23 supported catalyst appeared to be unsuitable for ODH owing to its negligible dehydrogenation selectivity. As regard ZSM5-80 supported catalyst, the DH and BD selectivity didn't

show such a clear tendency, it recorded the maximum DH and BD selectivity of 20% and 12% at O_2/n-C_4H_{10}=2, then decreased to almost 4% at feed ratio of 4.

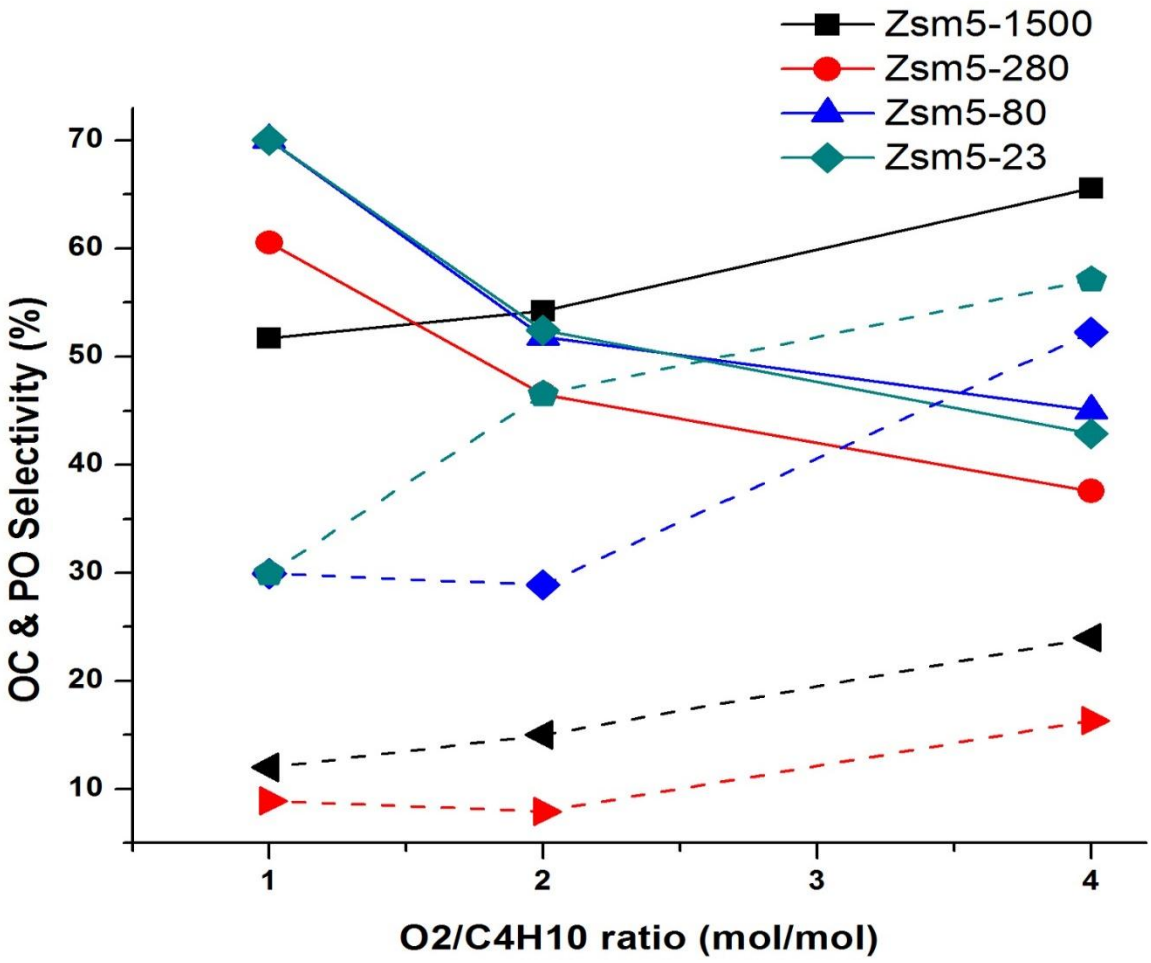

Figure 6 Influence of O_2/n-C_4H_{10} ratio on Oxygenate/Cracking (OC) and Partial Oxidation (PO) selectivity represented by (__) and (- - - -) respectively. Catalyst: 30 wt%Bi-20 wt%Ni supported on ZSM5 with Si/Al ratio of 23, 80, 280 and 1500.

The formation of oxygenate/cracking products exhibited a decreasing trend over ZSM5-280 ZSM5-80 and ZSM5-23 with increasing of O_2/n-C_4H_{10} ratio. An opposite trend was observed over ZSM5-1500. The PO selectivity increased with an increase of O_2/n-C_4H_{10} over ZSM5-1500 and ZSM5-23 supported catalysts. Regarding the ZSM5-280 and ZSM5-80 supported catalysts, the PO selectivity showed a slight decline when the O_2/n-

C_4H_{10} ratio increased from 1 to 2 mol/mol, then a significant increase was observed at feed ratio of 4.

4.1.2.2 Reaction Temperature:

The influence of reaction temperature on the catalytic performance was explored over different supported catalysts. In addition, a detailed investigation on reaction pathway was carried out over Bi-Ni/TiC by varying the reaction temperature from 350 to 500 ºC with step size of 50 ºC. Fig.2 presents the influence of temperature on catalyst activity and selectivity to various products. The conversion of n-butane was observed reasonably well at high reaction temperature, where it reached the maximum of 18.4% at 500 ºC. However, the dehydrogenation selectivity not only to butenes but also to butadiene exhibited the maximum value at 400 ºC, further increase in temperature, a diminishing trend in butenes and butadiene selectivity was observed. Whereas the formation of oxygenate and cracking (OC) products grew in second order curve, indicating higher activation energy of cracking compared to dehydrogenation. The selectivity towards partial oxidation remained at low level with slight decrease at higher reaction temperature. These results is in line with our previous work [39], indicating the partial oxidation (PO) and cracking reaction (OC) takes place separately on concentrated oxygen sites and activated oxygen sites respectively.

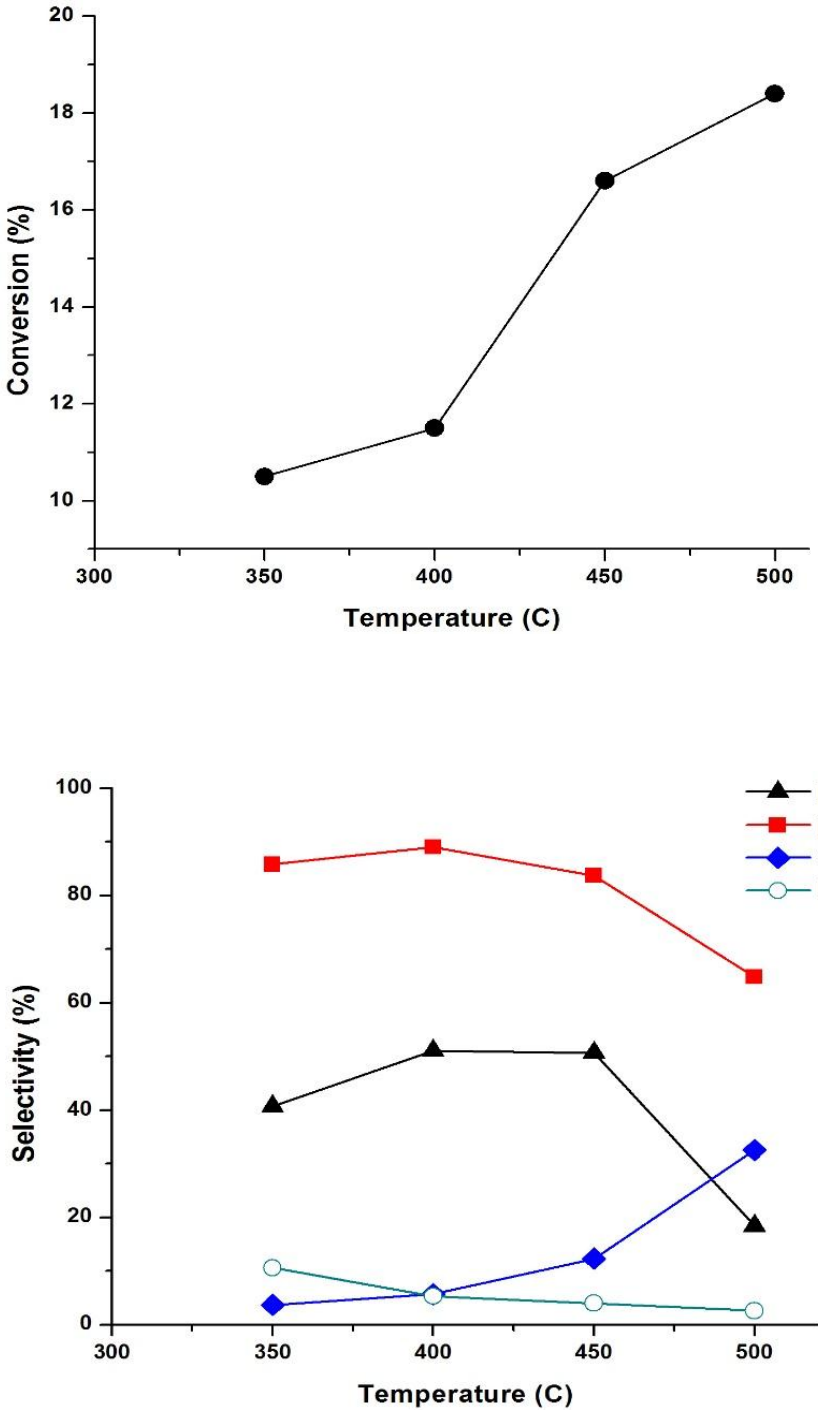

Figure 7 Influence of temperature on conversion and selectivity. Catalyst:30 wt%Bi-20 wt%Ni /TiC, O_2/n-C_4H_{10}=2 (mol mol^{-1})

Table 13 Effect of temperature on catalytic performance. Catalyst:30 wt%Bi-20 wt%Ni /SiC, O_2/C_4H_{10}=2

Temperature	**400**	**450**	**500**
n-C_4H_{10} conversion [%]	9.6	15.1	19.3
Selectivity*[1] [C%]			
DH	**88.6**	**87.3**	**79.4**
1-C_4H_8	44.3	34.9	30.4
BD	**14.8**	**27.1**	**25.7**
OC	9.4	10.6	18.2
PO	1.9	2.1	2.4
BD/DH %	16.7	31.0	32.4
(1-C_4H_8 + BD)/DH %*[2]	66.7	71.0	70.7
BD/(1-C_4H_8 + BD) %*[3]	25.0	43.7	45.8
BD yield	1.4	4.1	5.0

In case of Bi-Ni /SiC catalyst, the conversion was observed reasonably well at high reaction temperature, where it reached the maximum of 18.4% at 500 ºC. The DH selectivity decreased with rise of temperature, while the BD selectivity reached the maximum of 27.1% at 450 ºC , afterwhich a slight decline was noticed at 500 ºC. The selectivity towards cracking products increased at high temperature. Whereas the formation of partial oxidation products remained at low levels. The selectivity to 1st step dehydrogenation maintained stability approximately at 70%

Table 14 Effect of temperature on catalytic performance. Catalyst:30 wt%Bi-20 wt%Ni /Silicalite, O_2/C_4H_{10}=2

Temperature	**400**	**450**	**500**
n-C_4H_{10} conversion [%]	9.5	12.4	16.9
Selectivity*[1] [C%]			
DH	**72.4**	**71.0**	**63.2**
1-C_4H_8	31.4	30.1	26.4
BD	**19.2**	**18.0**	**16.3**
OC	23.7	24.0	30.9
PO	3.9	5.0	5.8
BD/DH %	26.5	25.4	25.8
(1-C_4H_8 + BD)/DH %*[2]	69.9	67.8	67.5
BD/(1-C_4H_8 + BD) %*[3]	37.9	37.4	38.2
BD yield	1.8	2.2	2.8

Concerning Bi-Ni /Silicalite, the conversion tends to increase with raising the reaction temperature. With rise of temperature, the dehydrogenation selectivity not only to butenes but also to BD declined. The formation of oxygenate/cracking products increased from 23.7% to 30.9% at 500 °C. The formation of PO products remained negligible. The selectivity to 1st and 2nd step dehydrogenation stayed constant at around 68% and 38% respectively.

Table 15 Effect of temperature on catalytic performance. Catalyst: 5%wt Co-5%wt Fe-10%wt Ni- 30%wt Bi/TiC, O_2/C_4H_{10}=2

Temperature	**400**	**450**	**500**
n-C_4H_{10} conversion [%]	7.2	11.1	15.8
Selectivity*[1] [C%]			
DH	**89.2**	**76.6**	**51.0**
1-C_4H_8	12.0	18.7	11.3
BD	**48.6**	**33.8**	**24.5**
OC	9.1	23.4	48.2
PO	1.7	0.0	0.7
BD/DH %	54.5	44.2	48.0
(1-C_4H_8 + BD)/DH %*[2]	67.9	68.6	70.0
BD/(1-C_4H_8 + BD) %*[3]	80.2	64.4	68.5
BD yield	3.5	3.8	3.9

Regarding 5%wt Co-5%wt Fe-10%wt Ni- 30%wt Bi/TiC catalyst, the conversion of n-butane rose to the maximum of 15.8% at 500 ℃. As expected, the DH and BD selectivity decreased considerably at high reaction temperature. The formation of oxygenate and cracked products dominates at high reaction temperature.

Table 16: Effect of temperature on catalytic performance. Catalyst: 10%wt Co -10%wt Ni- 30%wt Bi/TiC, O_2/C_4H_{10}=2

Temperature	**400**	**450**	**500**
n-C_4H_{10} conversion [%]	11.6	16.0	21.4
Selectivity*[1] [C%]			
DH	**84.5**	**65.1**	**42.5**
1-C_4H_8	13.7	10.7	5.0
BD	**43.5**	**37.9**	**28.2**
OC	15.5	34.9	56.7
PO	0.0	0.0	0.7
BD/DH %	51.5	58.3	66.3
(1-C_4H_8 + BD)/DH %*[2]	67.7	74.7	78.1
BD/(1-C_4H_8 + BD) %*[3]	76.1	78.0	84.9
BD yield	5.1	6.1	6.0

Regarding 10%wt Co -10%wt Ni- 30%wt Bi/TiC, the conversion rose from 11.6% at 400 °C to 21.4% at 500 °C. As expected, the formation of butenes and BD decreased whereas the cracking selectivity increased with rise of temperature. The PO selectivity remained negligible.

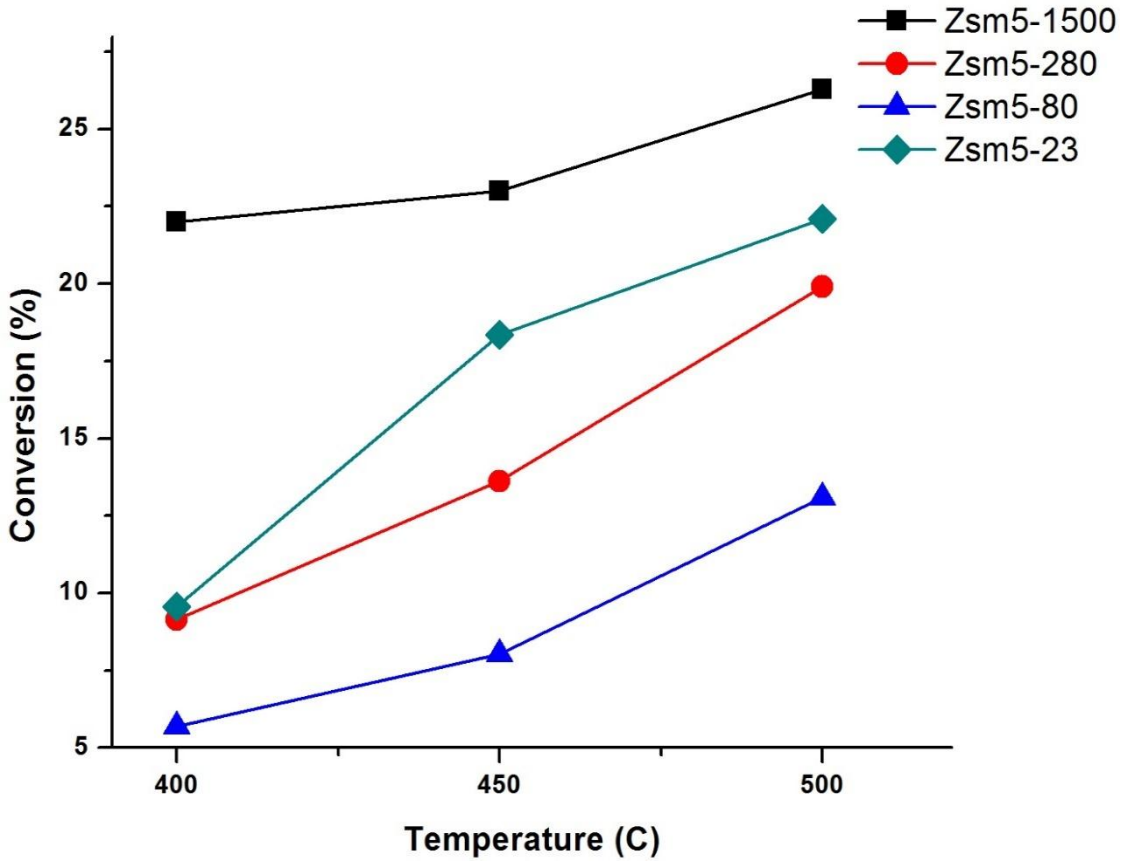

Figure 8 Effect of temperature on butane conversion. Catalyst: 30 wt%Bi-20 wt%Ni supported on ZSM5 with Si/Al ratio of 23,80, 280 and 1500 at O_2/C_4H_{10}=2.

The influence of temperature on butane conversion for bimetallic 30% Bi-20% Ni catalyst supported on ZSM5 with different Si/Al ratio was shown in Fig 8. As expected, the conversion increased with rise of temperature for all ZSM5 supported catalysts. The butane conversion followed the sequence: ZSM5-1500 > ZSM5-23 > ZSM5-280 > ZSM5-80.

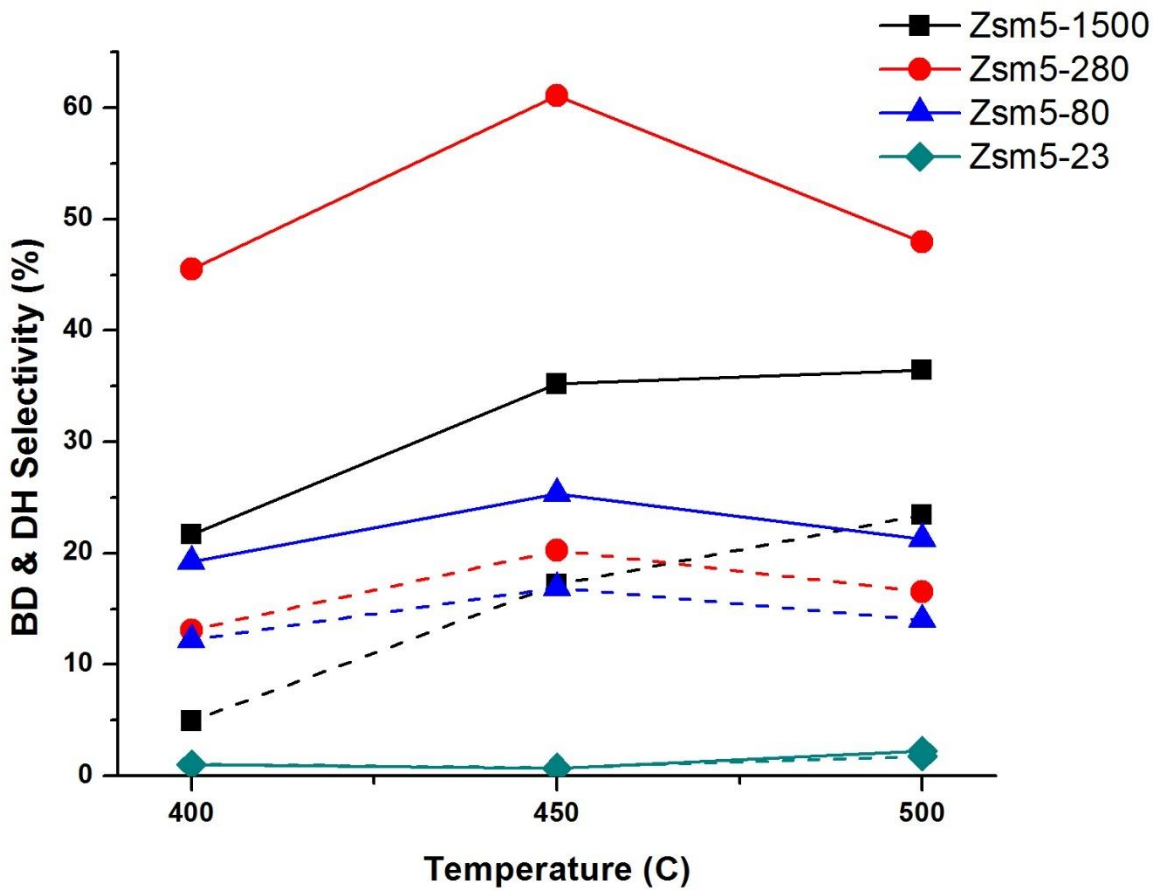

Figure 9 Effect of temperature on Dehydrogenation (DH) and Butadiene (BD) selectivity represented by (__) and (- - - -) respectively. Catalyst: 30 wt%Bi-20 wt%Ni supported on ZSM5 with Si/Al ratio of 23,80, 280 and 1500 at O_2/C_4H_{10}=2.

Fig 9 presents the effect of temperature on DH and BD selectivity. Both BD and DH selectivity showed a volcano shape over ZSM5-80 and ZSM5-280 supported catalysts. ZSM5-23 supported catalyst seemed to be unsuitable for ODH because of its negligible DH selectivity. Concerning, ZSM5-1500 supported catalyst, both DH and BD selectivity with raising the reaction temperature, it recorded the maximum DH and BD selectivity of 35% and 22% at temperature of 500 °C.

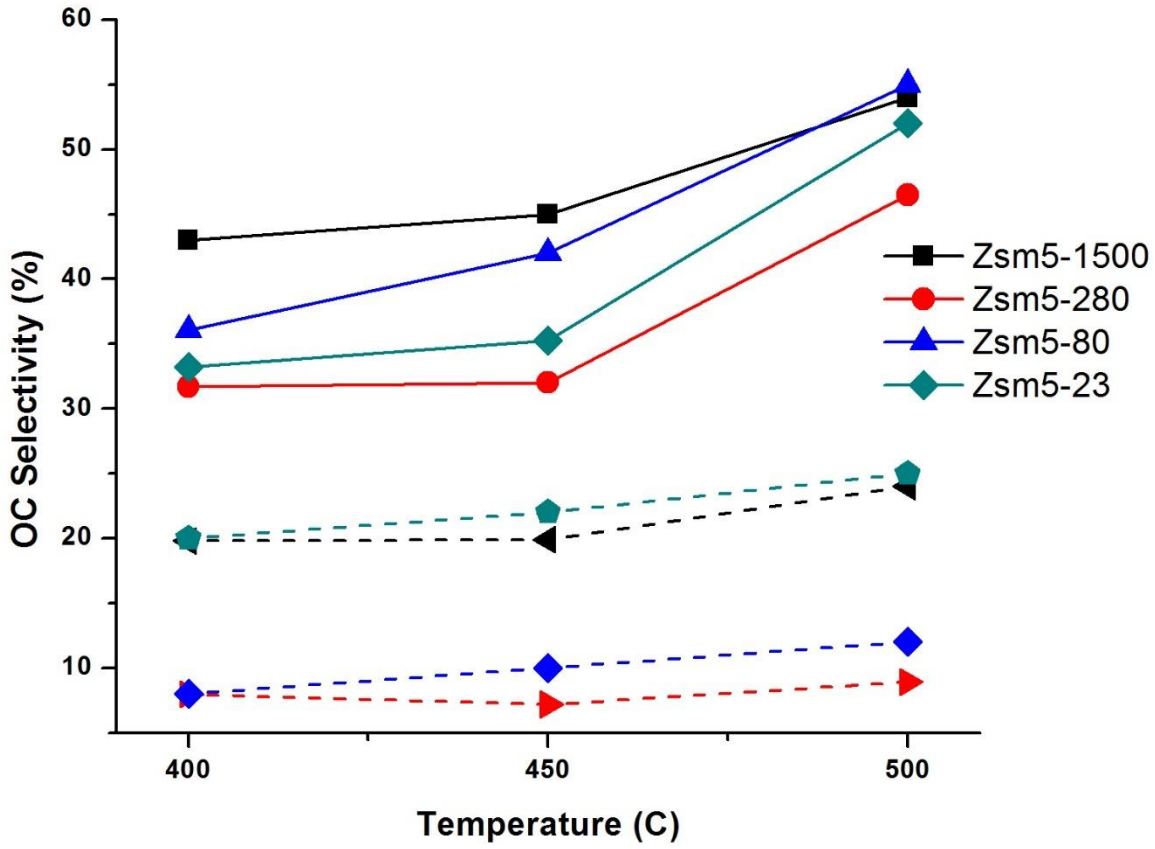

Figure 10 Effect of temperature on Oxygenate/Cracking (OC) and Partial Oxidation (PO) selectivity represented by (__) and (- - - -) respectively. Catalyst: 30 wt%Bi-20 wt%Ni supported on ZSM5 with Si/Al ratio of 23,80, 280 and 1500 at O_2/C_4H_{10}=2.

The formation of oxygenate/cracking products dominates at higher reaction temperature over all ZSM5 supported catalysts as shown in Fig 10. No significant increase was observed in PO selectivity with rise of temperature.

4.1.3 Effect of metal Composition

The influence of metal composition on the performance of Bi-Ni/TiC and Bi-Ni/Silicalite catalyst for oxidative dehydrogenation of n-butane to butadiene in the optimum reaction condition of 450 ºC and O_2/n-C_4H_{10} = 2.0 is represented in the following tables.

Table 17 Effect of Ni-Bi composition on catalytic performance. Catalyst: Bi-Ni/TiC, Reaction conditions: O_2/n-C_4H1_0 = 2.0, 450 ºC.

Metals Loading	**30Bi-20Ni**	**37.5Bi-20Ni**	**60Bi-20Ni**	**10Bi-20Ni**
n-C_4H_{10} conversion [%]	16.6	16.7	7.0	12.1
Selectivity*[1] [C%]				
DH	**83.7**	**78.3**	**83.6**	**67.6**
1-C_4H_8	13.6	19.0	13.0	8.8
BD	**50.7**	**37.4**	**38.4**	**41.3**
OC	12.3	18.8	9.2	11.2
PO	4.0	2.9	7.2	21.1
BD/DH %	60.6	47.8	46.0	61.1
(1-C_4H_8 + BD)/DH %*[2]	76.9	72.0	61.5	74.2
BD/(1-C_4H_8 + BD) %*[3]	78.9	66.3	74.8	82.4
BD yield	8.4	6.2	2.7	5.0

The effects of bismuth loading over TiC varied as 10, 30, 37.5 and 60 wt.% at fixed Ni loading on the butane conversion and products selectivity was investigated. Table 17 revealed that the butane conversion increased from12.1% to 16.7% when the Bi loading was increased from 10 to 37.5 wt%, further increase of Bi loading to 60 wt% resulted in a decline in butane conversion. Regarding the products distribution, the DH selectivity improved with Bi loading from 10 to 30 wt%, while it kept nearly constant as the Bi loading increased from 30 to 60 wt%. The 30Bi-20Ni/TiC exhibited the highest BD

selectivity with negligible selectivity of cracking. The PO selectivity tends to decrease with an increase in Bi loading, pointing out that Bi metal suppressed the partial oxidation reaction, this result is in accordance of our previous work [39].

Table 18 Effect of Ni-Bi composition on catalytic performance. Catalyst: Bi-Ni/Silicalite, Reaction conditions: O_2/n-C_4H_{10} = 2.0, 450 °C

Metals Loading	**30Bi-20Ni**	**20Bi-10Ni**	**60Bi-20Ni**	**10Bi-20Ni**
n-C_4H_{10} conversion [%]	12.4	8.9	12.6	9.1
Selectivity*[1] [C%]				
DH	**71.0**	**69.5**	**81.9**	**76.5**
1-C_4H_8	30.1	32.1	36.0	30.9
BD	**18.0**	**13.3**	**22.4**	**16.3**
OC	24.0	20.6	13.1	16.6
PO	5.0	9.9	5.0	6.9
BD/DH %	25.4	19.1	27.3	21.3
(1-C_4H_8 + BD)/DH %*[2]	67.8	65.3	71.3	61.7
BD/(1-C_4H_8 + BD) %*[3]	37.4	29.3	38.3	34.5
BD yield	2.2	1.2	2.8	1.5

Table 21 revealed that the conversion tends to increase with an increase of Bi loading from 10 to 60 wt.% at fixed Ni loading of 20 wt%. Considering products selectivity, the DH selectivity over 60Bi-20Ni/TiC was the highest. As regard the BD selectivity, it showed a clear tendency to increase with an increase in Bi loading. The OC selectivity didn't show a clear dependence on Bi loading, while the PO selectivity remained at low level in all catalysts investigated.

4.1.4 Ternary and Quaternary Metal Catalyst

The Co and Fe metal were combined with binary metals to form ternary and quaternary metal catalysts by substituting partially the 50% of Nickel in 20Ni-30Bi/TiC catalyst as shown in Table 22. These metal were combined with Bi and Ni in order to study their effect on the catalytic performance.

Table 19 Comparison of catalytic performance for ternary metal 10% Co-10% Ni- 30%Bi /TiC and quaternary metal 5%Co-5%Fe-10%Ni-30%Bi/TiC catalyst, Reaction condition: O_2/n-C_4H_{10} = 2.0, 450 ºC.

Catalyst	**5Co-5Fe-10Ni-30Bi**	**10Co-10Ni-30Bi**
n-C_4H_{10} conversion [%]	11.1	16.0
Selectivity*[1] [C%]		
DH	**76.6**	**65.1**
1-C_4H_8	18.7	10.7
BD	**33.8**	**37.9**
OC	23.4	34.9
PO	0.0	0.0
BD/DH %	44.2	58.3
(1-C_4H_8 + BD)/DH %*[2]	68.6	74.7
BD/(1-C_4H_8 + BD) %*[3]	64.4	78.0
BD yield	3.8	6.1

The conversion over 10Co-10Ni-30Bi/TiC was improved compared to binary metal 20Ni-30Bi/TiC catalyst, owing to high surface area of Co and easy accessibility to active sites [43]. Addition of Fe metal, resulted in lower conversion but the main DH selectivity improved due to the redox ability of Fe metal [43]. The BD selectivity showed a slight decline with addition of Fe metal resulting in high selectivity towards butenes i.e. 1st

dehydrogenation selectivity. The partial oxidation products weren't observed over both ternary and quaternary metal catalysts. The OC selectivity is higher over 10Co-10Ni-30Bi/TiC compared to quaternary metal catalyst, indicating that the cracking reaction is favorable over this catalyst. The formation of cracked products over quaternary metal catalyst was reduced due to an increase of catalyst basicity.

4.1.5 Effect of Space Velocity

The space velocity is an essential parameter in catalytic reactions that deserves further investigation. The influence of space velocity (6000, 8000 & 12000 mL/g. h) is shown in Fig.11 for Bi-Ni/TiC as the best catalyst candidate, at 450 ºC and O_2/n-C_4H_{10} ratio of 2. As expected, the n-butane conversion exhibited a slight decrease with an increase of the gas hourly space velocity (GHSV). This trend was ascribed to the fact that reaction contact time was shorten with an increase of space velocity. A similar 1,3-butadiene selectivity was observed when the gas hourly space velocity is varied from 6000 to 8000 mL/g. h (50.7% to 49.8 % respectively). However, further increase in GHSV from 8000 to 12000 mL/g. h resulted in a decrease of butadiene selectivity to 46%, pointing out that dehydrogenation to butadiene is a slow reaction, so it is favorable at low GHSV. On the other hand, the butenes selectivity monotonically increased with rise of GHSV, suggesting that dehydrogenation towards butenes is a relatively fast reaction. The selectivity of oxygenate formation partially followed by cracking was concomitantly suppressed as GHSV increases.

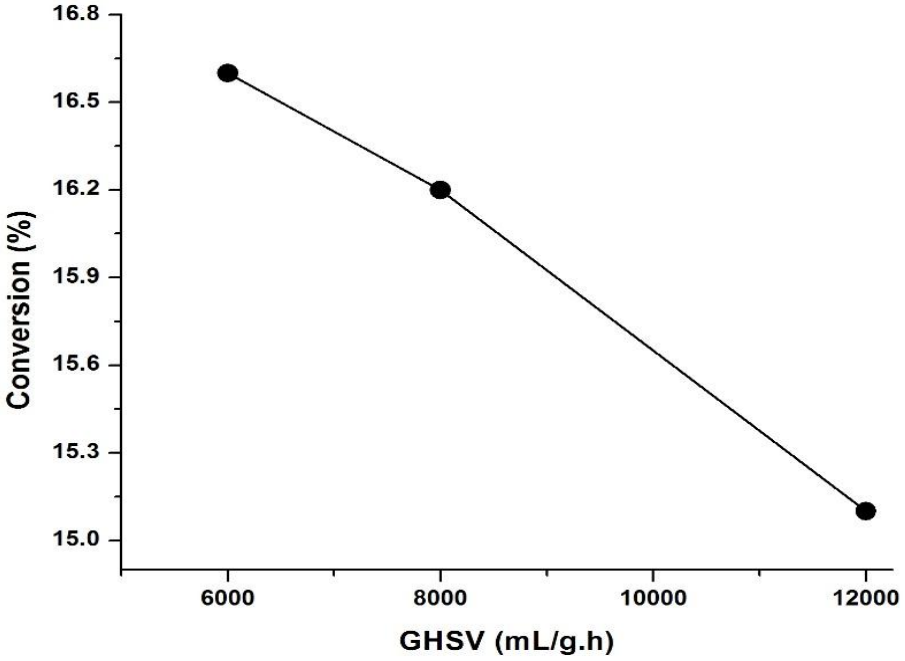
16.8
16.5
16.2
15.9
15.6
15.3
15.0
Conversion (%)
6000
8000
10000
12000
GHSV (mL/g.h)

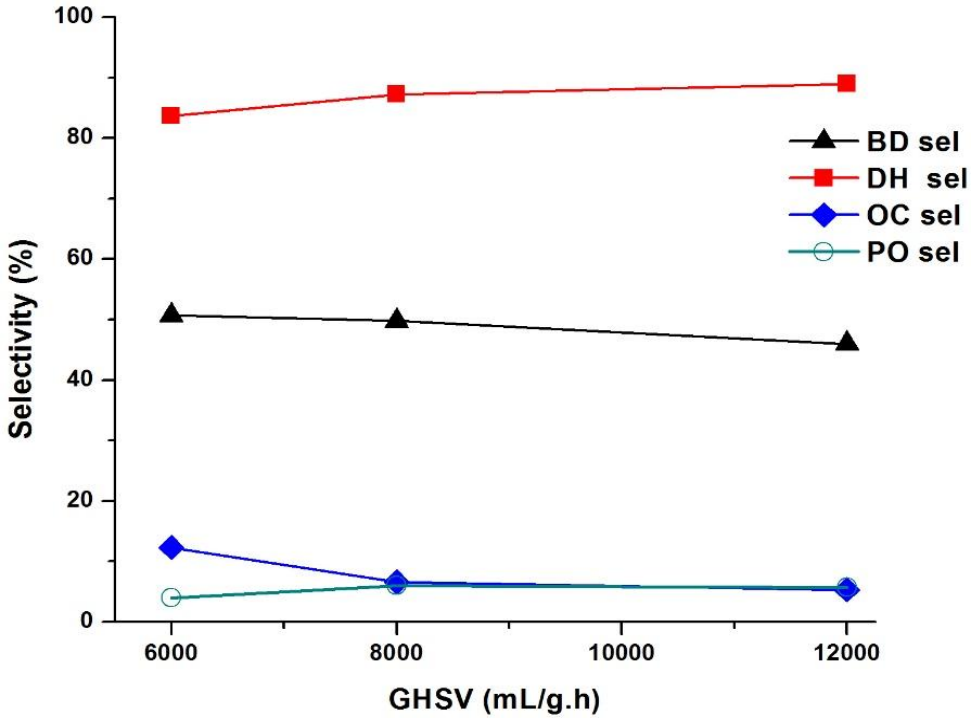

Figure 11 Effect of gas hourly space velocity (GHSV) on conversion and selectivity. Catalyst:30 wt%Bi-20 wt%Ni /TiC, O_2/n-C_4H_{10}=2 (mol mol^{-1}), 450 °C.

4.2 1-Butene and 2-butenes as feedstock

The catalytic performance in the case of using 1-butene and 2-butenes as feedstock was determined over Bi-Ni/TiC catalyst. Experiments were conducted at reaction temperature of 450 °C and O_2/C_4H_8 = 2. The result is shown in Table 20.

As evident from Table 20, Butadiene has the highest selectivity among dehydrogenated products for the case of n-butane feedstock. 1-butene selectivity followed BD with 13.6 %, whereas the selectivity to trans-2-butene and cis-2-butene was 10.4% and 9.0% respectively. When feeding the reactor with 1-butene, selectivity for BD around 74.4% was found while the selectivity for cis-2-butene and trans-2-butene was10.5% and 11.1% respectively. The formation of trans-2-butene and cis-2-butene when 1-butene was used

feedstock, indicates that isomerization reaction readily takes place. The molar ratio trans-2-butene/cis-2-butene is constant at 1 for both cases of n-butane and 1-butene feedstocks. Lopez Nieto et al. [44] reported that for catalysts with basic character, this molar ratio is close to 1. When the reactor is fed with 2-butenes (cis/trans = 50/50), most of it was converted to BD with selectivity of 91.4%, whereas a low percentage was isomerized to 1-butene. The OC and PO selectivity remained at negligible level when 1-butene and 2-butenes were used as feedstocks. As regards intermediate feedstocks, 2-butene is more reactive than 1-butene which is why it resulted in higher yield of BD.

Table 20 Comparison of catalytic performance using n-butane,1-butene and 2- butenes (cis/trans = 50/50) as feedstock for Bi-Ni/TiC catalyst. Reaction conditions: 450 °C, O_2/C_4 =2.0.

Feedstock	**n-butane**	**1-butene**	**2-butene**
Conversion [%]	16.6	59.5	74.7
Selectivity[*1] [%]			
DH	83.7	96	99.6
1-$C_4^=$	13.6	-	8.2
trans-2-$C_4^=$	10.4	11.1	-
cis-2-$C_4^=$	9.0	10.5	-
BD	50.7	74.4	91.4
OC	12.3	1.8	0
PO	4.0	2.2	0.4

BD yield	8.4	44.2	68.3

*1 DH: dehydrogenation, OC: oxygenate and the cracked, BD: 1,3-butadiene, PO: partial oxidation

4.3 Catalyst Stability

The catalytic stability of Bi-Ni/TiC catalyst was examined at 450 °C and O_2/n-C_4H_{10} = 2 for 10 h time of stream and results were depicted in Fig.12. In general, the catalyst exhibited a stable performance with time on stream. The n-butane conversion showed an approximate constant trend with little decline. The butadiene selectivity exhibited a slight decrease at initial reaction times and thereafter almost constant. The selectivity towards dehydrogenation and oxygenate formation were almost maintained at about their initial values; whereas the partial oxidation selectivity increased slightly. Major losses in dehydrogenation selectivity would render the catalyst unsuitable for industrial use. However, the Bi-Ni/TiC catalyst seems to preserve its ability to selectively convert n-butane to dehydrogenated products with time on stream.

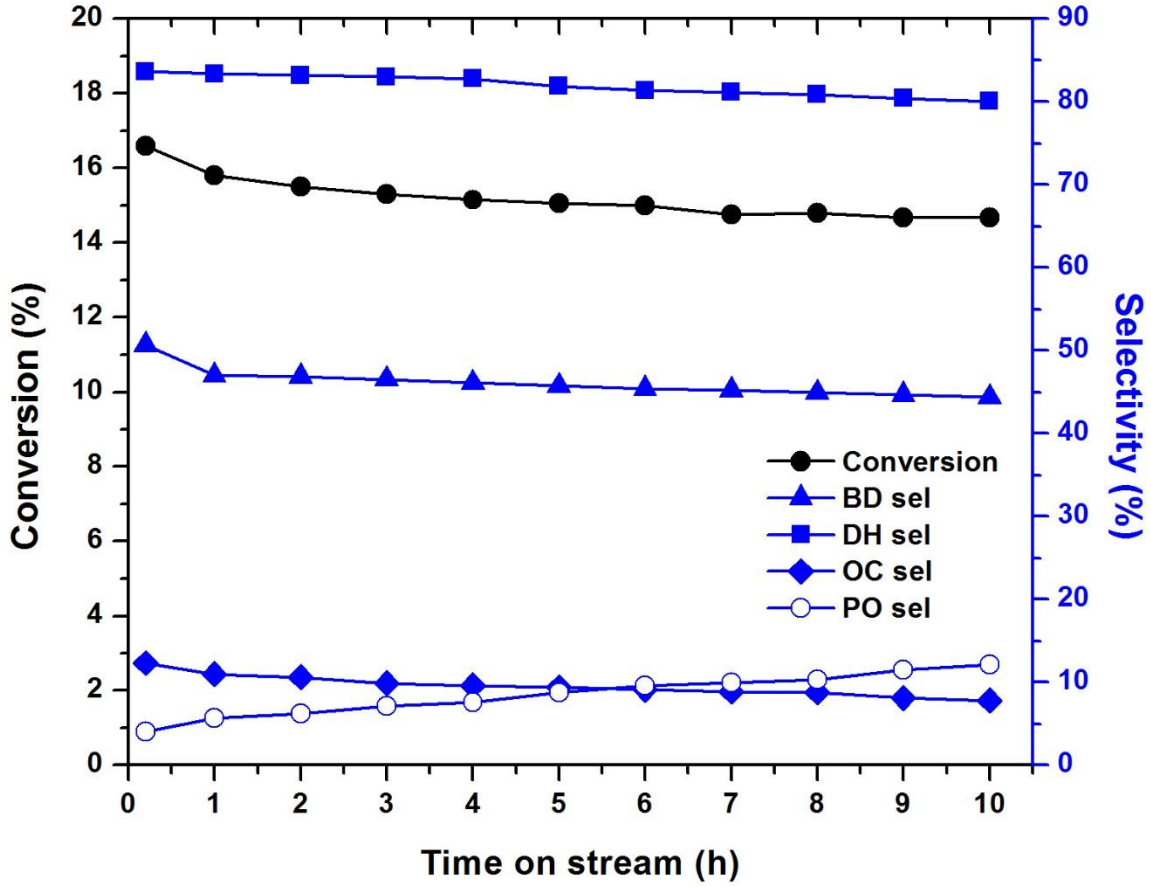

Figure 12 Stability of 30 wt%Bi-20 wt%Ni /TiC catalyst with time on stream.

4.4 Catalyst Characterization

4.4.1 Surface area and pore structure.

Different physico-chemical techniques were utilized to study the properties of the catalysts with the sole aim of determining the nature of the active sites and their interaction/dispersion with the different supports. BET and pore surface area, pore volume, and average pore diameter of various supports i.e TiC, SiC, Silicalite and none (without support) are shown in Table 21 The metal species only ($NiO\text{-}Bi_2O_3$) has BET surface area of 16 m^2/g-catalyst (25 m^2/g-support: equivalent to catalyst with support). All the supported catalysts contain the same amount of metal oxide species (20 wt% Ni

and 30 wt% Bi), hence their comparison was made based on the weight of the supports as presented in Table 21.

Table 21 Physical properties of catalysts and supports.

Catalyst: (Support)	BET surface area		Pore surface area		Pore volume		Average pore diameter
	[m^2/g-catalyst]	[m^2/g-support]	[m^2/g-catalyst]	[m^2/g-support]	[cm^3/g-catalyst]	[cm^3/g-support]	[nm]
TiC	20	32 (29)	17	27 (20)	0.11	0.18 (0.13)	27.1 (26.2)
SiC	05	09 (05)	04	06 (03)	0.06	0.10 (0.05)	65.4 (66.2)
Silicalite	173	275 (308)	75	119 (119)	0.06	0.10 (0.08)	3.3 (2.7)
none	16	25	14	22	0.22	0.35	62.9

() values for the support only.

TiC supported catalyst showed a BET and pore surface area values of 32 and 27 m^2/g-TiC which are higher compared to the only TiC support, 29 and 20 m^2/g respectively. The catalyst with SiC support also showed the same pattern even though the values are lower compared to TiC supported catalyst. The TiC catalyst also showed relatively high values of pore volume, 0.18 ml/g-TiC equivalent to 0.13 ml/g for the support while the SiC supported catalyst gave a lesser pore volume of 0.10 ml/g-SiO_2. Surface areas of catalysts are expected to be lower than that of the support mainly due to partial or total blockage of pores [45] Contrarily, both TiC and SiC supported catalysts showed an additional surface area and pore volumes resulting from the nickel and bismuth oxides

species impregnation. This kind of expansion is mainly due to super-impregnation by nano-crystallized metal oxides in nano-sized pores.

The Silicalite catalyst showed higher surface area than TiC and SiC catalysts with the values 275 and 119 m^2/g-silicalite for BET and pore surface area which are comparable with that of silicalite support with values of 308 and 119 m^2/g for BET and pore surface area respectively. Silicalite has an MFI zeolite structure containing a combination of SiO_2-Al_2O_3, hence showed similar effect with the two oxides for both before and after metal oxides species impregnation [43].

4.4.2 X-ray diffraction

The XRD patterns of catalysts with 20 wt% Ni-30 wt% Bi-O metal oxides over different support species of TiC, SiC, silicalite and none (without support) combined together are presented in Fig.13

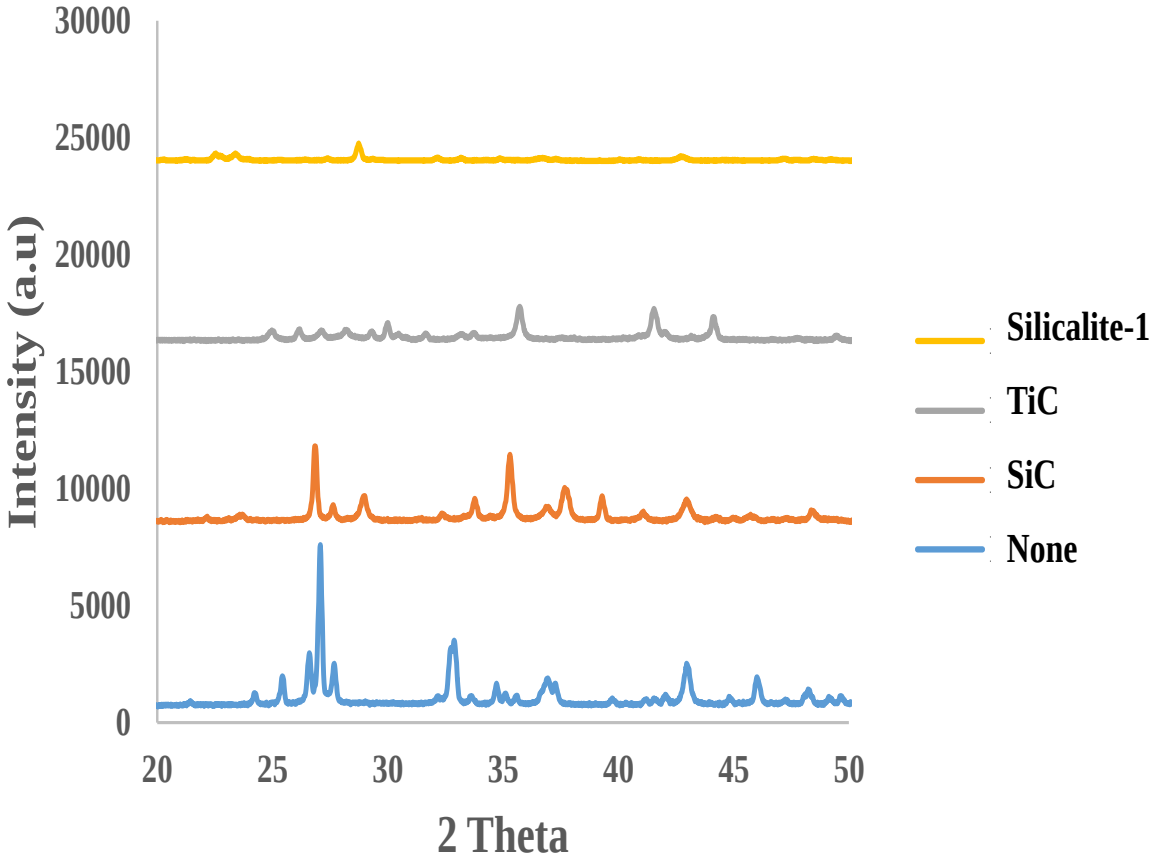

Figure 13 XRD patterns for catalysts of 20 wt% Ni-30 wt% Bi-O over different supports: SiC, TiC and MFI silicalite support.

All the catalysts showed some level of crystallinity eventhough it decreases in the order none > BNT > BNS > BNSilicalite. The XRD pattern of the metal species without support (none) showed a highly crystalline peak around 2θ = 27.1° and 32.9° which corresponds to monoclinic alpha-Bi_2O_3 which is less active and selective for butadiene formation [6]. Also, peaks around 2θ = 37° and 43° were observed which depicts NiO peaks [46]. This is an indication that effective combination of metal oxides was not achieved as large crystallites of both oxides were observed. This also agrees with the low BET surface area value reported above. The alpha-Bi_2O_3 phase serves as an active oxygen supplier selective for oxygenate and cracked products formation which is in agreement with the catalytic activity and selectivity results in Table 5. For the TiC supported catalyst, NiO peaks were not observed indicating high dispersion on the support. Broad peaks of low intensities were observed around 2θ = 25-30° which is a region typical of Bi_2O_3 phase [6]This is an indication of high dispersion of the metal species on the TiC support. The broadening of peaks usually signifies high dispersion on the support with much smaller sizes and crystallites [47] . A peak around 2θ = 29° was also observed which corresponds to the region of mixed metal oxide solid solution of NiO-Bi_2O_3 which serves as oxygen supplier for selective butadiene formation. Highly crystalline peaks around 2θ = 35 and 42° indicating reflections of TiC support FCC structure was observed [47]. For SiC supported catalyst, peak around 2θ = 35.6° was observed which corresponds to the hexagonal silicate phases of beta-SiC [45]. Highly crystalline phase of beta-Bi_2O_3 was also observed around 2θ = 27° which serve as oxygen supplier selective for the formation of butadiene while NiO which are mostly more highly dispersed on the support only showed a very low intensity peak around 2θ = 44°.

Silicalite supported catalyst has the least crystallinity relative to the other catalysts. It has peaks of 2θ = 7-10° and 22-25° which corresponds to the peaks of zeolite MFI structure [48]. Also, a crystalline $NiO\text{-}Bi_2O_3$ solid solution phase was observed at 2θ = 28-29° which also plays role as oxygen supplier for high dehydrogenation selectivity.

4.4.3 Temperature programmed reduction (TPR)

Reduction-oxidation (redox) property of a catalyst plays an important role in its activity and selectivity. The extent of active species reducibility is measured using TPR. The increase in active species reducibility accelerates the redox cycle thereby improving the catalyst activity. H_2-TPR patterns of Ni-Bi-O supported on TiC, SiC, MFI silicalite and none (metal species without support) is shown in Fig. 12. The TPR profiles were divided into three parts: i) easily reducible (350-550^oC) ii) moderately reducible (550-650^oC) and iii) difficult reducible (650-850^oC) with total as shown in Table 22 to ease discussions.

Figure 14 H2-TPR study for catalysts of 20 wt% Ni-30 wt% Bi-O over different supports: SiC, TiC and MFI silicalite support.

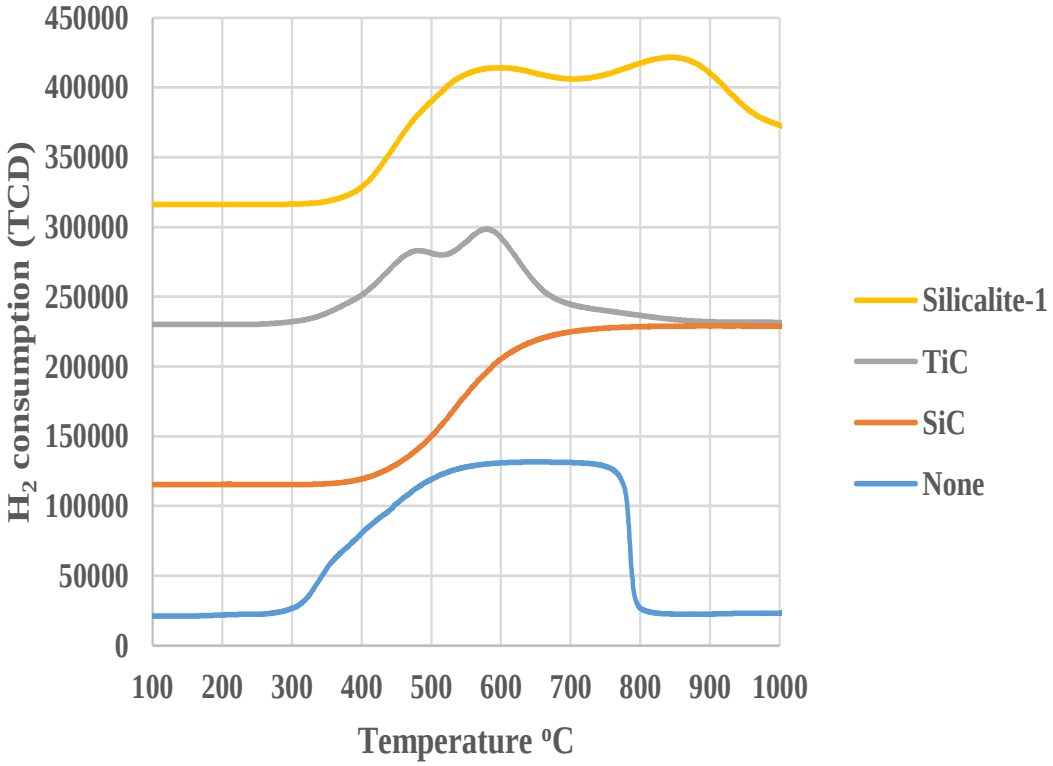

The active species reduction behavior on Al_2O_3 was previously reported [6]. Two NiO reduction peaks at 500-650 ^oC and Ni-Bi-O reduction peak at 700 ^oC were observed. It was concluded that the NiO species of such sample remain steadily as an active one and gave high BD selectivity and low OC selectivity. TiC supported catalyst showed peaks at even lower reduction temperatures of 450 ^oC and 575 ^oC indicating the ease of reducibility of the active species. This is related also to the state of NiO and Bi_2O_3 coordination on the support. SiC supported catalyst showed a broad reduction peak that extends from 600 ºC up to 1000 ^oC. SiC is highly stable and has an inert surface that is unreactive even at higher temperatures. This is an indication that the metal species reducibility is not really influenced by SiC support which is also why it gave a pattern similar to the unsupported metal species only.

Table 22 H_2 consumption in TPR: temperature programmed reduction of 20 wt% Ni-30 wt% Bi-O/support catalysts.

Catalyst support	TPR H_2 consumption [m mol/g]

Reduction temperature range	I (350-550 ºC)	II (550-650 ºC)	III (650-850 ºC)	total
TiC	3.72	3.63	-	7.35
SiC	-	4.95	4.95	9.90
Silicalite	-	4.51	6.63	11.14
none	1.47	1.00	1.31	3.78

The case of MFI silicalite also showed two main peaks at 600 ^{o}C and 850 ^{o}C with an increased H_2 consumption relative to the other supported catalysts. The increase in the reduction temperature is an indication of the strong interaction of smaller particles of Bi_2O_3 with the support surface. This also plays a great role in the formation of high oxygenate and cracking products.

4.4.4 Temperature programmed desorption (CO_2/NH_3)

The basic and acidic sites presents in the various supported catalysts were measured using CO_2- and NH_3-TPD respectively. The obtained values for catalysts 20 wt% Ni-30 wt% Bi-O metal oxides over different support species: TiC, SiC, MFI silicalite and none (only metal oxide species) are presented in Table 23. The basic sites are required for terminal H abstraction from n-butane and 1-butene intermediate while the acidic sites are necessary for 1-butene intermediate adsorption. All the profiles for both CO_2-TPD and NH_3-TPD were decomposed into three peaks signifying weak, moderate and strong base or acid respectively. The CO_2/NH_3 desorption temperatures are centered at ca. 170 ^{o}C, ca.

300 ^{o}C and ca. 400 ^{o}C for bases and 100-250 ^{o}C, 250-400 ^{o}C and 400 ^{o}C < for acid and are designated with I, II and III respectively. All the supported and unsupported catalysts showed both basic and acidic sites. The total amount of CO_2 desorbed that signifies total basic sites present is in the order: TiC > MFI silicalite > SiC > none, and the acid sites for both total, weak and moderate which signifies also the amount of NH_3 desorbed is: TiC > MFI silicalite > SiC > none. The balance of acidity to basicity which signifies the ratio of acidic to basic sites is in the order: MFI silicalite > SiC > TiC > none.

Table 23 Temperature programmed desorption analysis (CO2- and NH3-TPD) of 20 wt% Ni-30 wt% Bi O/support catalysts.

Catalyst (support)	Base amount with CO_2-TPD [mmol/g]*[1]				Acid amount with NH_3-TPD [mmol/g]*[2]			
	I	II	III	Total	I	II	III	Total
TiC	0.030	0.016	0.066	0.112	0.039	0.027	-	0.066
SiC	0.023	-	-	0.023	0.014	-	-	0.014
Silicalite	0.051	0.011	0.016	0.078	0.040	0.003	0.023	0.066
none	0.019	0.010	-	0.020	0.002	-	-	0.002

*[1] I (170^{o}C peak), II (300^{o}C peak), III (400^{o}C peak). *[2] I (100-250^{o}C), II (250-400^{o}C), III (>400^{o}C).

For the case of TiC supported catalyst, it showed high total basic sites (also high strong basic sites) with weak and moderate acid sites thus giving overall low total acidity/basicity ratio. This facilitates selective 1-butene intermediate adsorption and dehydrogenation to butadiene [43]. 1-butene adsorption by weak acid sites is necessary

for active 2nd step dehydrogenation without gaseous phase desorption which is why the catalyst gave low 1-butene selectivity. SiC supported catalyst has only weak acid and basic sites with high total acidity/basicity ratio. This is responsible for its high 1st step dehydrogenation selectivity but with overall low butadiene selectivity because there are no moderate/strong basic sites that can facilitate 2nd step dehydrogenation. Hence, it desorbs high amount of 1-butene into the gas phase without adsorption. MFI silicalite catalyst on the other hand gave the highest total acidity/basicity ratio. The strong acid sites present in the catalyst significantly affects both 1st and 2nd step dehydrogenation selectivities with high OC" selectivity on the contrary. 1-butene was also selectively desorbed into the gaseous phase leading to very low BD selectivity. It can be concluded that the different supports play significant role in acidity/basicity ratio balance of the catalysts with determine the overall BD production.

4.5 Kinetic Modelling Of n-Butane ODH Over 30Bi-20Ni/TiC

4.5.1 Model Development

In this section, a comprehensive kinetic model for oxidative dehydrogenation of n-butane over 30% Bi-20% Ni/TiC catalyst was developed by applying power law. A good kinetic model should contain low reaction steps as well as kinetic parameters but sufficient to describe the basic features of the reaction under study. Oxidative dehydrogenation of n-butane to butadiene has many reactions steps including consecutive and side reactions, this were simplified by lumping all cracked products which are methane, ethane, ethene, propane and propene as one entity. Also, butene isomers (1-butene, cis-2-butene and trans-2-butene) were also considered as one entity" (C4 olefin). Partial oxidation scheme that produces CO and H2 were detected in very small quantities, hence neglected.

The following Scheme was proposed which involves dehydrogenation and cracking of

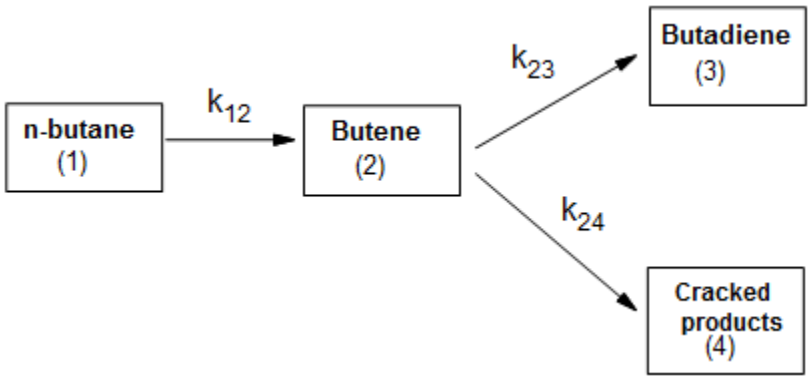

Scheme 2: Possible reaction scheme of ODH of n-butane along with cracking reaction over 30Bi-20Ni/TiC catalyst.

butenes as shown below;

It is worth noting that cracked products are mainly produced from n-butane as depicted in scheme.2, but in the proposed scheme the cracking products were considered to be produced by cracking of butenes intermediate, this scheme makes sense due to the fact that it is easier to crack olefins than paraffins especially at low reaction temperature.

The notation used in the scheme will be used along this report, the notation includes:

A≡ n-butane,

B ≡ Butene,

C ≡ Butadiene,

D ≡Cracked products

Table 24 Products distribution of n-butane ODH over 30Bi-20Ni/TiC catalyst.

Temperature (°C)	Contact Time (g.cat *min/g)	Mole Fraction				
		Conversion	y n-butane (out)	y butadiene	y butenes	y cracked
350	50.4	0.06	0.94	0.0215	0.0352	0.0002
	63	0.078	0.922	0.024	0.0409	0.0003
	75.6	0.0886	0.9114	0.0384	0.0459	0.0004
	88.2	0.097	0.903	0.0465	0.0501	0.0005
	100.8	0.115	0.885	0.0556	0.0538	0.0006
400	50.4	0.0774	0.9226	0.0289	0.0431	0.0012
	63	0.0989	0.9011	0.0393	0.0495	0.0016
	75.6	0.1139	0.8861	0.0502	0.0549	0.002
	88.2	0.12	0.88	0.0617	0.0593	0.0025
	100.8	0.152	0.848	0.0736	0.062	0.0029
450	50.4	0.0958	0.9042	0.0364	0.0484	0.0043
	63	0.117	0.883	0.05	0.0546	0.0058
	75.6	0.141	0.859	0.06	0.0595	0.0074
	88.2	0.165	0.835	0.0755	0.0633	0.0091
	100.8	0.181	0.819	0.0908	0.0645	0.0108
500	50.4	0.1096	0.8904	0.0425	0.0474	0.013
	63	0.138	0.862	0.0568	0.0517	0.0174
	75.6	0.1625	0.8375	0.0685	0.0546	0.0219
	88.2	0.189	0.811	0.0845	0.0562	0.0265

	100.8	0.215	0.785	0.102	0.0569	0.0313

From the design equation of Fixed Bed Tubular Reactor

$$-r_i = \frac{dF_i}{dW} \ldots\ldots\ldots\ldots\ldots\ldots\ldots\ldots\ldots\ldots\ldots\ldots\ldots (1)$$

$$F = \upsilon_o Ci \ldots\ldots\ldots\ldots\ldots\ldots\ldots\ldots\ldots\ldots\ldots\ldots\ldots (2)$$

$$\tau = w/F_{Tm} \ldots\ldots\ldots\ldots\ldots\ldots\ldots\ldots\ldots\ldots\ldots\ldots\ldots (3)$$

$$Ci = \frac{y_i F_{Tm}}{MW_i x \upsilon_o} \ldots\ldots\ldots\ldots\ldots\ldots\ldots\ldots\ldots\ldots\ldots (4)$$

Yi, Ci and MW" represent mass fraction, concentration, molecular weight of specie i respectively.

The rate equations for the different lumps can be deduced from the reaction network and with the help of suggested assumptions. So the rate equations for each lump can be written as:

Rate of disappearance of n-butane, r_A;

$$-r_A = -\frac{dC_A}{d\tau} = k_1 C_A \ldots\ldots\ldots\ldots\ldots\ldots\ldots\ldots\ldots\ldots\ldots\ldots\ldots (5)$$

Rate of appearance and disappearance of butene intermediate, r_{Bu};

$$r_B = \frac{dC_B}{d\tau} = (k_1 C_A - k_2 C_B^{0.75} - k_3 C_B^{0.75}) \ldots\ldots\ldots\ldots\ldots\ldots\ldots\ldots\ldots\ldots (6)$$

Rate of appearance of butadiene, r_C;

$$r_C = \frac{dC_C}{d\tau} = k_2\, C_B^{0.75} \quad \text{……………………………………(7)}$$

Rate of appearance of cracked products, r_D;

$$r_D = \frac{dC_D}{d\tau} = k_3\, C_B^{0.75} \quad \text{……………………………………(8)}$$

Recalling Eq.(4), the concentration can be written in terms of weight fraction, hence the equations can be reformulated in terms of fractions as:

Rate of disappearance of n-butane, r_A;

$$-r_A = -\frac{dY_A}{d\tau} = k_1\, C_A * MW_A \quad \text{……………………………………(9)}$$

Rate of appearance and disappearance of butene intermediate, r_B;

$$r_B = \frac{dY_B}{d\tau} = (k_1\, C_A - k_2\, C_B^{0.75\ 2} - k_3\, C_B^{0.75}) * MW_B \quad \text{……………………(10)}$$

Rate of appearance of butadiene, r_C;

$$r_C = \frac{dY_C}{d\tau} = k_2\, C_B^{0.75} * MW_C \quad \text{……………………………………(11)}$$

Rate of appearance of cracked products, r_D;

$$r_D = \frac{dY_D}{d\tau} = k_3\, C_B^{0.75} * MW_D \quad \text{……………………………………(12)}$$

The activation energy Ei is related to the temperature dependent rate constants ki according to the Arrhenius equation:

$$k_j = k_{oj} \exp\left[\frac{-Ej}{RT}\right] \quad \text{……………………………………(13)}$$

For reducing the parameter interaction, pre-exponential factor Ai could be replaced by the

K_{oi} and the expression of k_i is given below

$$k_i = k_{i0} \exp\left(-\frac{E_i}{R}\left(\frac{1}{T}-\frac{1}{T_0}\right)\right) \quad \text{.....(14)}$$

Where, k_{i0} and E_i are the pre-exponential factor and activation energy of the reaction i, respectively, T_0, the centering temperature (average of all the temperatures), since the experimental runs were performed at 350, 400, 450, and 500 °C, T_a was calculated as 450 °C.

$$k_{12} = k_{0,12} \exp\left(-\frac{E_{12}}{R}\left(\frac{1}{T}-\frac{1}{T_0}\right)\right) \quad \text{.....(15)}$$

$$k_{23} = k_{0,23} \exp\left(-\frac{E_{23}}{R}\left(\frac{1}{T}-\frac{1}{T_0}\right)\right) \quad \text{.....(16)}$$

$$k_{24} = k_{0,24} \exp\left(-\frac{E_{24}}{R}\left(\frac{1}{T}-\frac{1}{T_0}\right)\right) \quad \text{.....(17)}$$

4.5.2 Model Assumptions

There are several reaction possibilities along with various suggested mechanisms and different steps involved. In order to simplify the model and ease the model development so reasonable parameter estimation can be achieved;" the following is assumed:

- Mass transfer limitation is negligible
- Negligible catalyst deactivation

- Isothermal reactor condition
- Excess gas phase oxygen, hence negligible conversion
- Effectiveness factor is unity

The proposed reactions order were found to give the best fitting with the experimental data.

4.5.3 Model Parameters

To determine the kinetic parameters, the reaction rate constants (Eq.15-17) were combined with the rate equations (Eq.9-12). The concentration of each chemical species was represented in terms of mass fraction using Eq.4. Then, the set ordinary differential equations (ODEs) were solved numerically combined with a least square fitting of the experimental n-butane ODH data. MATLAB ODE 45 (fourth order Runge-Kutta method) was employed in solving the ODEs, while the model parameters were determined using Least Square Curve Fitting (lsqcruvefit subroutine). In order to obtain more reliable model, the n-butane ODH experiments were carried out at four different reaction temperatures (350-500 ºC) and five different contact time (50 -100 gcat min/g.butane). In this fashion, 20 data points were used for to estimate the parameters. Therefore, 6 model parameters were estimated with a degree of freedom of 14. The sufficient experimental data used in determination of kinetic parameters provides high accuracy of model results.

The following model discrimination criteria was considered:

1. The kinetic parameters (activation energy and specific reaction rates) must be positive and consistent to physical principles.
2. Correlation coefficient (R^2) closer to unity.

3. Lower sum of square residuals (SSR).
4. Smaller confidence intervals for each model parameter.

Table.25 lists the estimated rate constants and activation energy for all reaction paths shown in Scheme.2. The estimated activation energy for dehydrogenation to butene (E12) and butadiene (E23) are 24 and 15 kJ/mol respectively, while the apparent activation energy for cracking (E24) is 105 kJ/mol. The second step dehydrogenation to butadiene requires the lowest activation energy (15 kJ/mol), pointing out the dehydrogenation to butadiene is energetically easy (Madeira et al., 1996). These results were expected since Bi-Ni/TiC catalyst is more selective for dehydrogenation to butadiene than other competing reactions as shown in Table 5. The cracking reaction presented the highest activation energy (E24) of 105 kJ/mol. This high activation energy of cracking is consistent with the low experimental value of cracking selectivity presented in Table 5. In the literature, the activation energies for n-butane oxidative dehydrogenation (either butene cracking or dehydrogenation to butene and butadiene) are scarce. L.M. Madeira et al. (Madeira et al., 1996) reported an activation energy of 16 kJ/mol for dehydrogenation to butadiene over Cs-doped NiMoO4 catalyst. Unfortunately, the activation energy for cracking is not available in the open literature. However, the value of our activation energy for cracking was found to be lower than the one reported by Babajide et al. (Ajayi et al., 2014) who obtained a cracking activation energy of 130 kJ/mol for catalytic dehydrogenation of n-butane over VO_x CrO_x /MCM‐41 catalyst.

Comparing the model predictions and experimental data, it can be seen from Fig. 15 that, *n*-butane conversion predicted by the model fits with the experimental results in

an excellent manner. Butadiene and butene yields exhibited an accurate match between model predictions and experimental data as depicted in Fig. 16 and Fig. 17.

Table 25 Estimated values of kinetic parameters at 95% confidence intervals.

Parameters	**Values**	**Model discrimination**	**Values**
$\mathbf{k_{1o}}$ **(**mL/g_{cat}. min**)**	2.25 ± 0.718	Correlation coefficient, R^2	0.9992
$\mathbf{K_{2o}}$ **(**$mol^{0.25}\, mL^{0.75}/g_{cat}$. min**)**	0.402 ± 0.034		
$\mathbf{K_{3o}}$ **(**$mol^{0.25}\, mL^{0.75}/g_{cat}$. min**)**	0.678 ± 0.0484		
$\mathbf{E_1}$ **(kJ/mol)**	24 ± 0.2		
$\mathbf{E_2}$ **(kJ/mol)**	15 ± 0.007		
$\mathbf{E_3}$ **(kJ/mol)**	130 ± 7.3		

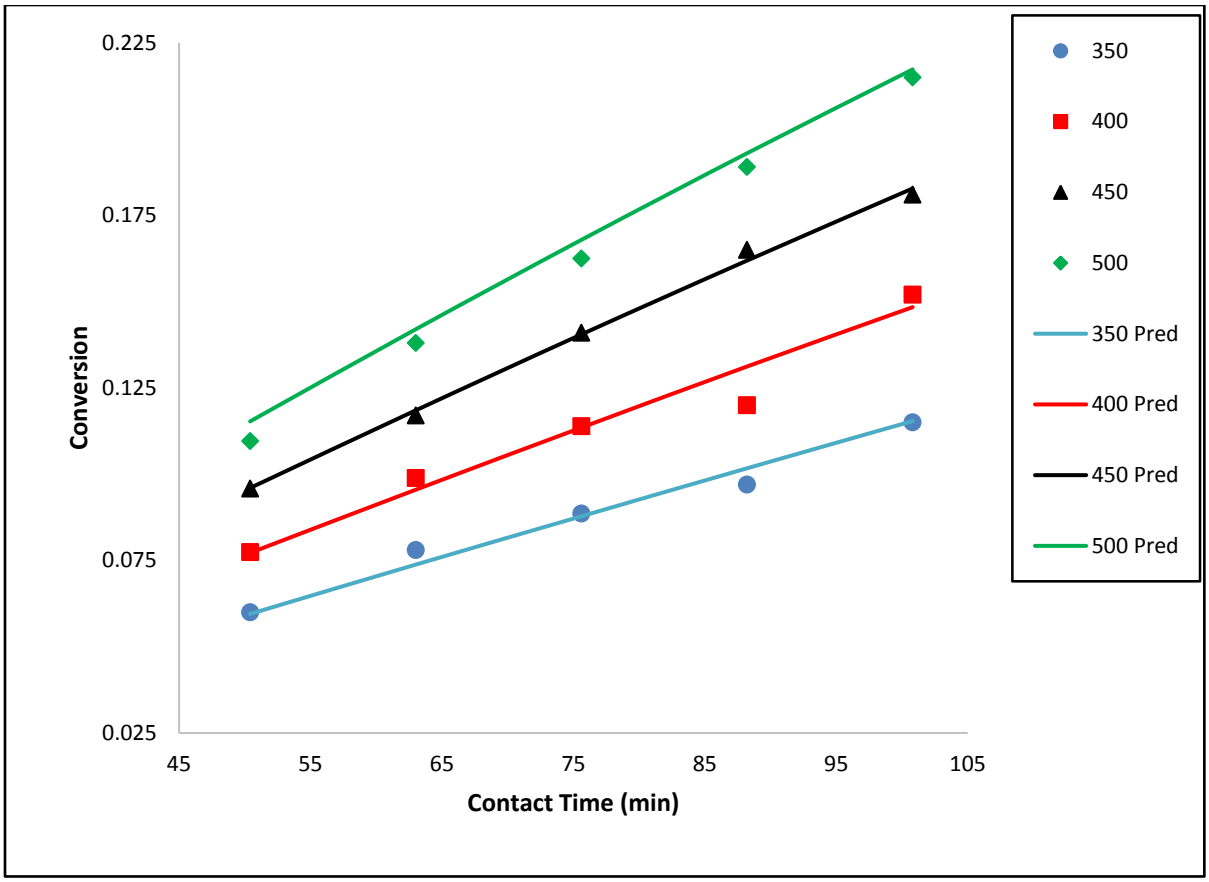

Figure 15 Comparison between predicted values and experimental data for n-butane conversion at various temperatures.

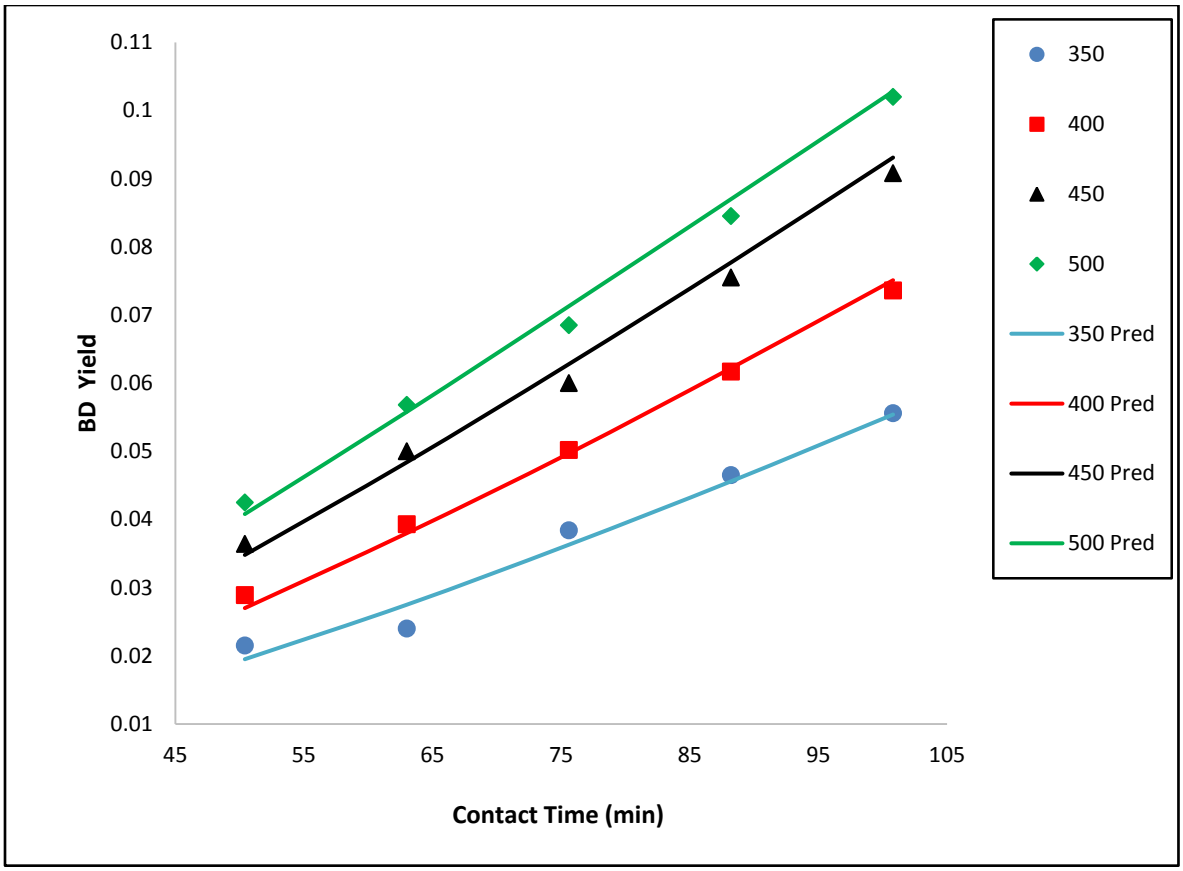

Figure 16 Comparison between predicted values and experimental data for butadiene yield at different temperatures.

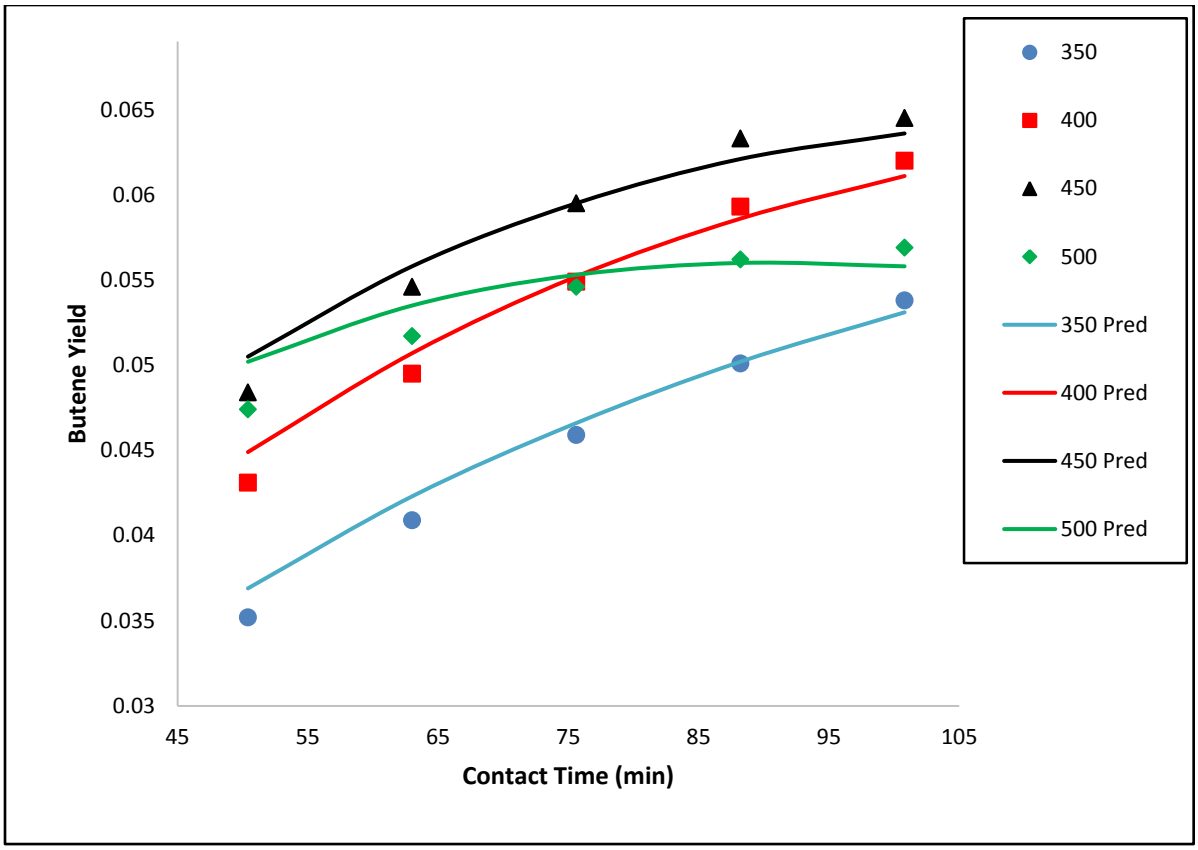

Figure 17 Comparison between model prediction and experimental results for butene yield at various temperatures

It can be concluded that the model reasonably predicts the ODH of n-butane over Bi-Ni/TiC" catalyst and also the model discrimination values of 0.9992 and 0.0071 for correlation coefficient (R^2)" and sum of squares respectively.

CHAPTER 5

CONCLUSIONS AND RECOMMENDATIONS

5.1 Conclusions

The influence of different supports such as TiC, SiC and silicalite on catalytic performance of bimetallic Bi-Ni oxide catalysts was explored. The catalysts were characterized by XRD, BET, CO_2/NH_3-TPD and H_2-TPR measurement techniques. As indicated by TPD, the nature of support species played a significant role in determining the acidity of the catalysts. Moreover, the presence of different supports influenced the reduction behavior of the catalysts. Large surface area is not the crucial factor deciding about the catalytic activity of supported catalysts. Much more essential are both redox property and acid-base character of the catalysts. The unsupported Bi-Ni catalyst presented the poorest catalytic activity coupled with the highest cracking selectivity. As regard the supported catalysts, the yield of dehydrogenated products (butenes & butadiene) followed the sequence: Bi-Ni/TiC > Bi-Ni/SiC > Bi-Ni/Silicalite. Concerning the Bi-Ni/TiC, a wide range of operating parameters were investigated, including reaction temperature, O_2/n-C_4H_{10} ratio and space velocity. The product selectivity was significantly influenced by the reaction temperature. Moderate temperature favors the formation of butenes and 1,3-butadiene, whereas, high temperature was also responsible for undesired cracking and partial oxidation reactions. The highest selectivity of dehydrogenated products was observed at 450°C, while cracking products dominates at 500°C. As regards the space velocity, the 1,3-butadiene selectivity decreased with an increase of GHSV, pointing out that dehydrogenation to butadiene is a slow reaction, so it

is favorable at low GHSV. O_2/n-C_4H_{10} ratio of 2 appears to be the best trade-off between high conversion and satisfactory dehydrogenation selectivity. The Bi-Ni/TiC catalyst exhibited satisfactory stability as proven by 10 hours on stream test, where no significant catalyst deactivation was observed. It was deduced that, the bimetallic Bi-Ni oxide catalyst loaded on TiC have high catalytic activity and selectivity for oxidative dehydrogenation of n-butane to butenes and 1,3-butadiene due to either redox property or a couple of strong basicity and weak acidity.

The kinetic model showed that among the reaction paths, the dehydrogenation of butene to butadiene has the lowest activation energy (15 kJ/mol), while highest activation energy of 105 kJ/mol is required for cracking reaction. These results were found to be in consistence with the experimental data of products selectivity.

5.2 Recommendations:

After sequential studies regarding the applicability of Bi-Ni catalyst supported on TiC, SiC & Silicalite for oxidative dehydrogenation of n-butane to 1,3-butadiene, the following recommendations can be advanced for future studies:

1. A Comprehensive study of partial oxidation and cracking reactions that happen as side reactions of oxidative dehydrogenation of n-butane should be conducted.
2. Other synthesis methods should be explored in order to determine which method will enhance the active interaction between the metal and support for better catalyst performance.

3. Other characterization techniques such SEM, Raman spectroscopy, FTIR, UV-vis, EDX should also be used in order to clearly reveal the active metal species interaction that led to the good performance of the improved catalyst.
4. Kinetic modeling based on molecular description is desired. This will give better insight on the role of metals loading on the reaction pathways for the production of 1,3-butadiene.

References

[1] "Butadiene Product Stewardship Guidance Manual, American Chemistry Council Olefins Panel, American Chemistry Council, 2001, Revised 2002."

[2] W. C. White, "Butadiene production process overview," *Chem. Biol. Interact.*, vol. 166, no. 1–3, pp. 10–14, 2007.

[3] R. Grabowski, "Kinetics of Oxidative Dehydrogenation of C 2 - C 3 Alkanes on Oxide Catalysts," *Catal. Rev.*, vol. 48, no. 2, pp. 199–268, 2006.

[4] D. Bhattacharyya, S. K. Bej, and M. S. Rao, "Oxidative dehydrogenation of n-butane to butadiene. Effect of different promoters on the performance of vanadium-magnesium oxide catalysts," *Appl. Catal. A, Gen.*, vol. 87, no. 1, pp. 29–43, 1992.

[5] S. A. Al-ghamdi, "Oxygen-Free Propane Oxidative Dehydrogenation Over Vanadium Oxide Catalysts : Reactivity and Kinetic Modelling," no. December, 2013.

[6] B. Rabindran Jermy, S. Asaoka, and S. Al-Khattaf, "Influence of calcination on performance of Bi–Ni–O/gamma-alumina catalyst for n-butane oxidative dehydrogenation to butadiene," *Catal. Sci. Technol.*, vol. 5, no. 9, pp. 4622–4635, 2015.

[7] I. C. Marcu, I. Sandulescu, and J. M. M. Millet, "Effects of the method of preparing titanium pyrophosphate catalyst on the structure and catalytic activity in

oxidative dehydrogenation of n-butane," *J. Mol. Catal. A Chem.*, vol. 203, no. 1–2, pp. 241–250, 2003.

[8] V. Murgia, E. M. F. Torres, J. C. Gottifredi, and E. L. Sham, "Sol-gel synthesis of V_2O_5-SiO_2 catalyst in the oxidative dehydrogenation of n-butane," *Appl. Catal. A Gen.*, vol. 312, no. 1–2, pp. 134–143, 2006.

[9] G. Neri, A. Pistone, S. De Rossi, E. Rombi, C. Milone, and S. Galvagno, "Ca-doped chromium oxide catalysts supported on alumina for the oxidative dehydrogenation of isobutane," *Appl. Catal. A Gen.*, vol. 260, no. 1, pp. 75–86, 2004.

[10] A. P. V. Soares, L. D. Dimitrov, M. C. R. A. De Oliveira, L. Hilaire, M. F. Portela, and R. K. Grasselli, "Synergy effects between ? and ? phases of bismuth molybdates in the selective catalytic oxidation of 1-butene," *Appl. Catal. A Gen.*, vol. 253, no. 1, pp. 191–200, 2003.

[11] U. P. De Valencia, "OXIDATIVE DEHYDROGENATION OF N-BUTANE OVER VMgO CATALYSTS," vol. 21, pp. 101–109, 2006.

[12] "Petroleum and Petrochemicals Economics Program: Petrochemical Market Dynamics: Butadiene Derivatives published by Nexant, 2012."

[13] "Oxidative dehydrogenation of butenes over Sn-P-O and Li-Sn-P-O catalysts." 1987.

[14] M. M. Bhasin, J. H. McCain, B. V. Vora, T. Imai, and P. R. Pujadó, "Dehydrogenation and oxydehydrogenation of paraffins to olefins," *Appl. Catal. A Gen.*, vol. 221, no. 1–2, pp. 397–419, 2001.

[15] A. A. Lemonidou, L. Nalbandian, and I. A. Vasalos, "Oxidative dehydrogenation

of propane over vanadium oxide based catalysts. Effect of support and alkali promoter," *Catal. Today*, vol. 61, no. 1, pp. 333–341, 2000.

[16] a Hakuli, M. E. Harlin, L. B. Backman, and a O. I. Krause, "Dehydrogenation of i-Butane on CrO_x / SiO_2 Catalysts," *J. Catal.*, vol. 184, pp. 349–356, 1999.

[17] M. L. Ferreira and M. Volpe, "On the nature of highly dispersed vanadium oxide catalysts: Effect of the support on the structure of VO(x) species," *J. Mol. Catal. A Chem.*, vol. 164, no. 1–2, pp. 281–290, 2000.

[18] F. Arena, F. Frusteri, A. Parmaliana, G. Martra, and S. Coluccia, *Oxidative dehydrogenation of propane on supported V2O5 catalysts. The role of redox and acid-base properties*, vol. 119. Elsevier Masson SAS, 1998.

[19] M. A. Vuurman, F. D. Hardcastle, and I. E. Wachs, "Characterization of CrO_3/Al_2O_3 catalysts under ambient conditions: Influence of coverage and calcination temperature," *J. Mol. Catal.*, vol. 84, no. 2, pp. 193–205, 1993.

[20] S. Derossi *et al.*, "Propane Dehydrogenation on Chromia/Silica and Chromia/Alumina Catalysts," *Journal of Catalysis*, vol. 148, no. 1. pp. 36–46, 1994.

[21] B. Y. Jibril, N. O. Elbashir, S. M. Al-Zahrani, and A. E. Abasaeed, "Oxidative dehydrogenation of isobutane on chromium oxide-based catalyst," *Chem. Eng. Process. Process Intensif.*, vol. 44, no. 8, pp. 835–840, 2005.

[22] B. P. Ajayi, B. Rabindran Jermy, B. A. Abussaud, and S. Al-Khattaf, "Oxidative dehydrogenation of n-butane over bimetallic mesoporous and microporous zeolites with CO_2 as mild oxidant," *J. Porous Mater.*, vol. 20, no. 5, pp. 1257–1270, 2013.

[23] B. Tope, Y. Zhu, and J. A. Lercher, "Oxidative dehydrogenation of ethane over

Dy2O3/MgO supported LiCl containing eutectic chloride catalysts," *Catal. Today*, vol. 123, no. 1–4, pp. 113–121, 2007.

[24] F. Cavani and F. Trifirò, "The oxidative dehydrogenation of ethane and propane as an alternative way for the production of light olefins," *Catal. Today*, vol. 24, no. 3, pp. 307–313, 1995.

[25] S. Gaab, M. Machli, J. Find, R. K. Grasselli, and J. A. Lercher, "Oxidative dehydrogenation of ethane over novel Li/Dy/Mg mixed oxides: Structure-activity study," *Top. Catal.*, vol. 23, no. 1–4, pp. 151–158, 2003.

[26] B. Fu, J. Lu, P. C. Stair, G. Xiao, M. C. Kung, and H. H. Kung, "Oxidative dehydrogenation of ethane over alumina-supported Pd catalysts. Effect of alumina overlayer," *J. Catal.*, vol. 297, pp. 289–295, 2013.

[27] E. Heracleous, M. Machli, A. A. Lemonidou, and I. A. Vasalos, "Oxidative dehydrogenation of ethane and propane over vanadia and molybdena supported catalysts," *J. Mol. Catal. A Chem.*, vol. 232, no. 1–2, pp. 29–39, 2005.

[28] "28- 268 [50," vol. 21, no. 2002, p. 2003, 2003.

[29] V. Murgia, E. Sham, J. C. Gottifredi, and E. M. F. Torres, "Oxidative dehydrogenation of propane and n-butane over alumina supported vanadium catalysts," *Lat. Am. Appl. Res.*, vol. 34, no. 2, pp. 75–82, 2004.

[30] B. M. Weckhuysen and D. E. Keller, "Chemistry, spectroscopy and the role of supported vanadium oxides in heterogeneous catalysis," *Catal. Today*, vol. 78, no. 1–4 SPEC., pp. 25–46, 2003.

[31] H. Armendariz *et al.*, "Oxidative dehydrogenation of n-butane on zinc-chromium ferrite catalysts," *J. Mol. Catal.*, vol. 92, no. 3, pp. 325–332, 1994.

[32] a. N. Vasil'ev and P. N. Galich, "Catalysts for the oxidative dehydrogenation of butenes and butane to butadiene," *Chem. Technol. Fuels Oils*, vol. 33, no. 3, pp. 185–192, 1997.

[33] Y. Xu, J. Lu, M. Zhong, and J. Wang, "Dehydrogenation of n-butane over vanadia catalysts supported on silica gel," *J. Nat. Gas Chem.*, vol. 18, no. 1, pp. 88–93, 2009.

[34] J. McGregor *et al.*, "The role of surface vanadia species in butane dehydrogenation over VOx/Al2O3," *Catal. Today*, vol. 142, no. 3–4, pp. 143–151, 2009.

[35] H. Lee *et al.*, "Effect of oxygen capacity and oxygen mobility of supported Mg 3(VO 4) 2 catalysts on the performance in the oxidative dehydrogenation of n-butane," *J. Ind. Eng. Chem.*, vol. 18, no. 2, pp. 808–813, 2012.

[36] J. K. Lee *et al.*, "Oxidative dehydrogenation of n-butane to n-butene and 1,3-butadiene over Mg 3(VO 4) 2/MgO-ZrO 2 catalysts: Effect of Mg:Zr ratio of support," *J. Ind. Eng. Chem.*, vol. 18, no. 3, pp. 1096–1101, 2012.

[37] B. Xu, X. Zhu, Z. Cao, L. Yang, and W. Yang, "Catalytic oxidative dehydrogenation of n-butane over V2O5/MO-Al2O3 (M = Mg, Ca, Sr, Ba) catalysts," *Chinese J. Catal.*, vol. 36, no. 7, pp. 1060–1067, 2015.

[38] J. M. L. Nieto, B. Solsona, R. K. Grasselli, and P. Concepción, "Promoted NiO catalysts for the oxidative dehydrogenation of ethane," *Top. Catal.*, vol. 57, no. 14, pp. 1248–1255, 2014.

[39] B. R. Jermy, B. P. Ajayi, B. A. Abussaud, S. Asaoka, and S. Al-Khattaf, "Oxidative dehydrogenation of n-butane to butadiene over Bi-Ni-O/γ-alumina catalyst," *J. Mol. Catal. A Chem.*, vol. 400, pp. 121–131, 2015.

[40] G. P. Heitmann, G. Dahlhoff, and W. F. Hölderich, “Catalytically Active Sites for the Beckmann Rearrangement of Cyclohexanone Oxime to ε-Caprolactam,” *J. Catal.*, vol. 186, no. 1, pp. 12–19, 1999.

[41] E. Heracleous, A. F. Lee, K. Wilson, and A. A. Lemonidou, “Investigation of Ni-based alumina-supported catalysts for the oxidative dehydrogenation of ethane to ethylene: Structural characterization and reactivity studies,” *J. Catal.*, vol. 231, no. 1, pp. 159–171, 2005.

[42] E. Heracleous and A. A. Lemonidou, “Ni-Nb-O mixed oxides as highly active and selective catalysts for ethene production via ethane oxidative dehydrogenation. Part II: Mechanistic aspects and kinetic modeling,” *J. Catal.*, vol. 237, no. 1, pp. 175–189, 2006.

[43] S. A.-K. G. Tanimu, B.R. Jermy , S. Asaoka, “Composition effect of metal species in (Ni, Fe, Co)-Bi-O/gamma-Al2O3 catalyst on oxidative dehydrogenation of n-butane to butadiene,” vol. 19, pp. 1858–1868, 2013.

[44] J. M. L. Nieto, P. Concepcion, a Dejoz, H. Knozinger, F. Melo, and M. I. Vazquez, “Selective oxidation of n-butane and butenes over vanadium-containing catalysts,” *J. Catal.*, vol. 189, no. 1, pp. 147–157, 2000.

[45] H. Romar *et al.*, “Characterisation and Catalytic Fischer-Tropsch Activity of Co-Ru and Co-Re Catalysts Supported on γ-Al2O3, TiO2 and SiC,” *Top. Catal.*, vol. 58, no. 14–17, pp. 887–895, 2015.

[46] A. Hameed, V. Gombac, T. Montini, M. Graziani, and P. Fornasiero, “Synthesis, characterization and photocatalytic activity of NiO-Bi2O3 nanocomposites,” *Chem. Phys. Lett.*, vol. 472, no. 4–6, pp. 212–216, 2009.

[47] L. Ma, S. Sui, and Y. Zhai, “Preparation and characterization of Ir/TiC catalyst for oxygen evolution,” *J. Power Sources*, vol. 177, no. 2, pp. 470–477, 2008.

[48] P. Arudra, T. I. Bhuiyan, M. N. Akhtar, A. M. Aitani, S. S. Al-khattaf, and H. Hattori, “Silicalite‐1 As E ffi cient Catalyst for Production of Propene from 1‐Butene,” 2014.

VITAE

Name	Omer Elmutasim Elmahadi Elfaki
Nationality	Sudanese
Date of Birth	14/05/1991
Email	omer.90@live.com
Address	B.5, Kafori, Khartoum, Sudan
Academic Background	Bachelor of Science, Chemical Engineering (2008-2013)
	University of Khartoum, Sudan